15ME742
TRIBOLOGY

<u>ATME COLLEGE OF ENGINEERING</u>

VISION

Development of academically excellent, culturally vibrant, socially responsible and globally competent human resources

MISSION

1. To keep pace with advancements in knowledge and make the students competitive and capable at the global level.
2. To create an environment for the students to acquire the right physical, intellectual, emotional and moral foundations and shine as torch bearers of tomorrow's society.
3. To strive to attain ever-higher benchmarks of educational excellence.

DEPARTMENT OF MECHANICAL ENGINEERING

VISION

To impart excellent technical education in mechanical engineering to develop technically competent, morally upright and socially responsible mechanical engineering professionals.

MISSION:

1. To provide an ambience to impart excellent technical education in mechanical engineering.

2. To ensure state of-the- art facility for learning, skill development and research in mechanical engineering.

3. To engage students in co-curricular and extra-curricular activities to impart social & ethical values and imbibe leadership quality.

PROGRAM EDUCATIONAL OBJECTIVES (PEO'S)

After successful completion of program, the graduates will be

PEO 1: Able to have successful professional career in the allied areas and be proficient to perceive higher education.

PEO2: Attain the ability to understand the need, technical ability to analyse, design and manufacture the product.

PEO 3: Work effectively, ethically and socially responsible in allied fields of Mechanical Engineering.

PEO 4: Work in a team to meet personal and organizational objectives and to contribute to the development of the society at large.

PROGRAM OUTCOMES (PO'S)

The Mechanical engineering program students will attain:

PO1.Engineering knowledge: Apply the knowledge of mathematics, science, engineering fundamentals, and an engineering specialization to the solution of complex engineering problems

PO2.Problem analysis: Identify, formulate, research literature, and analyze complex engineering problems reaching substantiated conclusions using first principles of mathematics, natural sciences, and engineering sciences

PO3.Design/development of solutions: Design solutions for complex engineering problems and design system components or processes that meet the specified needs with appropriate consideration for the public health and safety, and the cultural, societal, and environmental considerations

PO4.Conduct investigations of complex problems: Use research-based knowledge and research methods including design of experiments, analysis and interpretation of data, and synthesis of the information to provide valid conclusions

PO5. Modern tool usage: Create, select, and apply appropriate techniques, resources, and modern engineering and IT tools including prediction and modeling to complex engineering activities with an understanding of the limitations

PO6.The engineer and society: Apply reasoning informed by the contextual knowledge to assess societal, health, safety, legal and cultural issues and the consequent responsibilities relevant to the professional engineering practice

PO7. Environment and sustainability: Understand the impact of the professional engineering solutions in societal and environmental contexts, and demonstrate the knowledge of, and need for sustainable development

PO8. Ethics: Apply ethical principles and commit to professional ethics and responsibilities and norms of the engineering practice

PO9. Individual and team work: Function effectively as an individual, and as a member or leader in diverse teams, and in multidisciplinary settings

PO10. Communication: Communicate effectively on complex engineering activities with the engineering community and with society at large, such as, being able to comprehend and write effective reports and design documentation, make effective presentations, and give and receive clear instructions

PO11. Project management and finance: Demonstrate knowledge and understanding of the engineering and management principles and apply these to one's own work, as a member and leader in a team, to manage projects and in multidisciplinary environments

PO12. Life-long learning: Recognize the need for, and have the preparation and ability to engage in independent and life-long learning in the broadest context of technological change

PROGRAM SPECIFIC OUTCOMES (PSO'S)

After successful completion of program, the graduates will be

PSO 1: To comprehend the knowledge of mechanical engineering and apply them to identify, formulate and address the mechanical engineering problems using latest technology in a effective manner.

PSO 2: To work successfully as a mechanical engineer in team, exhibit leadership quality and provide viable solution to industrial and societal problems.

PSO 3: To apply modern management techniques and manufacturing techniques to produce products of high quality at optimal cost.

PSO 4: To exhibit honesty, integrity, and conduct one responsibly, ethically and legally, holding the safety and welfare of the society paramount

TRIBOLOGY

Course	Code	Credits	L-T-P	Assessment		Exam Duration
				SEE	CIA	
TRIBOLOGY	15ME742	03	3-0-0	80	20	3 Hrs

Course objectives:

1. Understand the fundamentals of tribology and associated parameters.
2. Apply concepts of tribology for the performance analysis and design of components experiencing relative motion.
3. Analyse the requirements and design hydrodynamic journal and plane slider bearings for a given application.
4. Select proper bearing materials and lubricants for a given tribological application.
5. Apply the principles of surface engineering for different applications of tribology.

MODULE -1
Introduction to tribology: Historical background, practical importance, and subsequent use in the field. Lubricants: Types and specific field of applications. Properties of lubricants,viscosity, its measurement, effect of temperature and pressure on viscosity, lubrication types, standard grades of lubricants, and selection of lubricants.
08 **Hours**

MODULE -2
Friction: Origin, friction theories, measurement methods, friction of metals and non-metals.
Wear: Classification and mechanisms of wear, delamination theory, debris analysis, testing methods and standards. Related case studies.

08 Hours

MODULE -3
Hydrodynamic journal bearings: Friction forces and power loss in a lightly loaded journal bearing, Petroff's equation, mechanism of pressure development in an oil film, and Reynold's equation in 2D. Introduction to idealized journal bearing, load carrying capacity, condition for equilibrium, Sommerfeld's number and it'ssignificance;partial bearings, end leakages in journal bearing, numerical examples on full journal bearings only.   **08 Hours**

MODULE -4
Plane slider bearings with fixed/pivoted shoe: Pressure distribution, Load carrying capacity, coefficient of friction, frictional resistance in a fixed/pivoted shoe bearing, center of pressure, numerical examples.
Hydrostatic Lubrication: Introduction to hydrostatic lubrication, hydrostatic step bearings, load carrying capacity and oil flow through the hydrostatic step bearing, numerical examples.   **08 Hours**

MODULE -5
Bearing Materials: Commonly used bearings materials, and properties of typical bearing materials. Advantages and disadvantages of bearing materials.
Introduction to Surface engineering: Concept and scope of surface engineering. Surface modification – transformation hardening, surface melting, thermo chemical processes. Surface Coating – plating,fusionprocesses, vapor phase processes. Selection of coating for wear and corrosion resistance.
                                                                                                08 **Hours**

List of Text Books:
1."Introduction to Tribology", B. Bhushan, John Wiley & Sons, Inc., New York, 2002
2. "Engineering Tribology", Prasanta Sahoo, PHI Learning Private Ltd, New Delhi, 2011.
3."Engineering Tribology", J. A. Williams, Oxford Univ. Press, 2005.

List of Reference Books:
1. "Introduction to Tribology in bearings", B. C. Majumdar, Wheeler Publishing.
2. "Tribology, Friction and Wear of Engineering Material", I. M.Hutchings, Edward Arnold, London,1992.
3. "Engineering Tribology", G. W. Stachowiak and A. W. Batchelor, Butterworth-Heinemann,1992.
4. "Friction and Wear of Materials", Ernest Rabinowicz, John Wiley & sons,1995.
5. "Basic Lubrication Theory", A. Cameron, Ellis Hardwoods Ltd., UK.
6. "Handbook of tribology: materials, coatings and surface treatments", B.Bhushan, B.K. McGraw-Hill,1997.

Module 1

Contents:

Introduction To Tribology: Historical Background,

Practical Importance, And Subsequent Use in the field.

Lubricants: Types and Specific Field of Applications.

Properties of Lubricants, Viscosity, Its Measurement,

Effect of Temperature and Pressure on Viscosity,

Lubrication Types,

Standard Grades of Lubricants, and Selection of Lubricants.

Objectives
1. Basics of tribology
2. Basics of lubricants and lubrication

1.1 INTRODUCTION

The word 'tribology' is derived from the Greek word *tribos* which means rubbing. So, the literal translation of the word is 'the science of rubbing'. Tribology is defined as *the science and technology of interacting surfaces in relative motion and of related subjects and practices*. The subject 'tribology' generally deals with the technology of lubrication, control of friction and prevention of wear of surfaces having relative motion under load. Tribology is the art of providing operational analysis to problems of great economic significance, namely, maintenance, reliability and wear of equipment starting from household appliances to spacecraft. To have a thorough understanding of the subject and its application to machine elements, it is necessary to have an in-depth knowledge in many areas such as chemistry of lubricants, physics of fluid flow, surface topography, contact mechanics, material science, mathematics and mechanical engineering. Thus, the subject is truly multi-disciplinary in nature.

1.2 HISTORY

Tribology as a subject is relatively new. But interest in the constituent parts of tribology is believed to be older than recorded history (Dowson, 1998). Our ancestors were concerned with reducing friction in translationary motion, and in this respect records show the use of wheels from 3500 BC. Drills were made during the Paleolithic period for drilling holes or producing fire and they were fitted with bearings made from bones or antlers. Potters' wheels or stones for grinding cereals clearly indicate the use and knowledge of some form of bearings. A tomb in Egypt provides evidences of the use of

lubricants. A chariot in the tomb still contains some of the original animal-fat lubricants in its wheel bearings. A ball-thrust bearing dated about 40 AD was found in Lake Nimi near Rome.

Leonardo da Vinci (1452–1519) first postulated a scientific approach to friction. He deduced the laws governing the motion of a rectangular block bearing over a flat surface and introduced the concept of coefficient of friction as the ratio of the friction force to normal load. But his work remained unpublished for a long time. In 1699, Guillaume Amontons rediscovered the laws and is usually credited with the discovery of the two laws. First, the friction force resisting sliding at the interface is directly proportional to the normal loads and, second, the friction force does not depend on the apparent area of contact. Later on Charles–Augustin Coulomb verified these laws and added a third one that the friction force is independent of velocity once motion starts. It was Coulomb who made a clear distinction between static friction and kinetic friction.

These three laws are still found in elementary texts on Physics and Engineering and are used today in many areas. Many other developments took place during the 1500s, particularly in the use of improved bearing-materials. In 1684, Robert Hooke suggested the use of contamination of steel shafts and bell-metal bushes as preferable to wood shod with iron for wheel bearings. In the later part of the 18th century, the growth of industrialization brought about further developments. Though essential laws of viscous flow were postulated by Newton in 1668, any scientific understanding of lubricated bearing operations did not occur until the end of the 19th century. The beginning of understanding of the principles of hydrodynamic lubrication was made possible with the experimental studies of Beauchamp Tower (1884) and theoretical interpretations of N.P. Petroff (1883) and Osborne Reynolds (1886). Since then the hydrodynamic bearing theory and practice has seen extremely rapid developments to meet the demand for reliable bearings in new machinery.

Wear is a much younger member in the tribology family than friction and bearing development. It was initiated on a largely empirical basis and scientific studies of wear developed only a little until the mid-20th century. Since the beginning of the 20th century, knowledge in all areas of tribology has expanded tremendously due to enormous industrial growth leading to demand for tribology. More recently, the emergence of proximal probes and high-capability computational techniques has allowed systematic investigations of interfacial problems with high resolution in micro- and nano-structures used in magnetic storage systems, micro-electromechanical systems (MEMS) and other industrial applications. These have led to the development of the new field of microtribology or nanotribology. This new member in the tribology family is concerned with experimental and theoretical investigations of processes ranging from atomic scale to microscales, occurring during adhesion, friction, wear and thin film lubrication at sliding surfaces.

1.3 INDUSTRIAL IMPORTANCE

Tribology is vital to modern machinery involving sliding and rolling surfaces. Brakes, clutches, bolts, nuts, driving wheels on automobiles, etc., use friction in a productive manner. Wear is also used in a productive manner in many cases, such as writing with a pencil, polishing, machining and shaving.

Unproductive friction and wear take place in engines, gears, cams, bearings and seals. It has been estimated that approximately one-third of the world's energy resources, in present use, appear as friction in one form or the other. Friction and wear usually cost money in the form of energy loss and material loss; can decrease national productivity; can affect national security and quality of life. Wear can also cause accidents. Thus, the knowledge of tribology can lead to various substantial and significant savings without deployment of large capital investment. Research in tribology leads to increased plant efficiency, fewer breakdowns, better performance and, above all, significant savings.

1.4   OIL LUBRICANTS

Any liquid having some amount of viscosity can be regarded as lubricant. At the same time, it should be as mobile as possible to remove heat and to avoid power loss due to viscous drag. It should be stable under thermal and oxidation stresses, have low volatility, good mechanical stability, etc.

Natural Organics

These include animal fat, whale oil, shark oil, vegetable oils, mineral oils, etc. Animal fats are naturally occurring esters formed by the combination of long chain organic acids with alcohols. Castor oil, rapeseed oil, etc. belong to vegetable oil category. These have low oxidation and thermal stability than mineral oils. They also have a tendency to break down to give sticky deposits. The

refining of petroleum produces mineral oils. They can be obtained for a range of viscosities: very mobile to very viscous. The chemical compounds making up mineral oils are mainly hydrocarbons of three types:

(a) Paraffins—open chain hydrocarbons

(b) Napthenes—closed ring hydrocarbons

(c) Aromatics—hydrocarbons based on benzene rings.

Oil is termed as paraffinic oil or napthenic oil depending on the majority percentage of paraffins or napthenes in it. The aromatics, though remain as a small percentage, play a vital role in boundary lubrication. Mineral oils can be used up to a maximum temperature of 200°C whereas animal and vegetables can be used up to a maximum temperature of 120°C.

Synthetic Organics

Synthetic organics have evolved as a result of the requirement of lubricants to be used at extreme temperatures, pressure, humidity, etc. These can be used up to a maximum temperature of 400°C. These include synthetic hydrocarbons, diesters, chlorofluoro-carbon, fatty acid esters, polyglycolether, fluoroester, phosphate ester, silicate ester, silicone, silane, polyphenyl ether, disiloxane, perfluoroalkyl polyether, etc. Synthetic hydrocarbons are prepared by the polymerization of specific olefin monomers and these can be prepared to optimize their viscosity-temperature, stability and volatility properties. Chlorofluorocarbons are chemically inert and have excellent thermal and oxidation stability but suffer from the drawbacks like poor viscosity-temperature properties, high-pour point, high volatility, etc. They are expensive and difficult to make and hence find only limited use. Esters, on the other hand, have excellent viscosity-temperature properties, volatility properties, good additive response to oxidative and lubrication behaviour. An enormous variety of esters is possible by the combination of different acids and alcohols. Fatty acid esters have moderately low volatility and low thermal and oxidation resistance. These are used in most magnetic tapes and floppy disk drives. Diesters or dibasic esters are commonly used in aircraft engines because of their better volatility characteristics than fatty acid esters. Neopentyl polyol esters are better than diesters in relation to thermal and oxidation stability and volatility. These are used as a gas turbine engine lubricant. Polyglycol ethers have very good thermal properties. Fluoroesters have good oxidation resistance but poor viscosity-temperature properties. Phosphate esters have excellent lubrication property and find wide use as anti-wear additives for petroleum and some other synthetic lubricants. Silicate esters have high- thermal stability, low viscosity and volatility but poor hydrolytic stability. These are mainly used for low-temperature corrosion prevention. Silicones have extreme chemical inertness, thermal stability but low volatility and surface tension. So these are ideal hydrodynamic lubricants. These are also used in various types of grease formulation for space use, these are very expensive and hence find limited use only in extreme operating conditions. Silanes have high-thermal stability compared to others. Polyphenyl ethers (PPE) have good thermal and oxidation resistance but poor volatility and viscosity properties. Perfluoropolyethers (PFPE) are

suitable for high-temperature applications, high vacuum, chemical resistance applications, etc.

GREASES

In fact, greases are oils that are thickened with solids (thickener) to form semi-fluid products. The type of thickener determines the characteristics of the grease. Greases are preferred to liquid lubricants in cases where the application of continuous supply of lubricant is not needed or there is no sufficiently tight enclosure to retain a liquid lubricant. They are very common in rolling element bearings, as the lubricating arrangement is very simple. They act as lubricant as well as seal dirt. But the use of greases is limited as they do not flow easily and cannot carry away the heat generated at high speed operations.

Thickeners compose 5 to 17 per cent of a simple grease formulation and control the characteristics of the product grease. The alkaline compounds are added and saponification occurs. The water produced from chemical reaction is boiled off. The amount of soap (thickener) formation depends on the amount of fatty acid and alkaline compound (generally metal hydroxide) used. The resulting thickening action is known as *consistency*, which is a measure of the hardness or softness of the grease. A variety of thickeners is used and accordingly properties of resulting grease are obtained. Water stabilized calcium soap is a variety based on calcium stearate stabilized with water. The grease with such thickener has excellent water resistance but its use is limited to about 80°C because of evaporation of stabilizing water at high temperature. Anhydrous calcium soap or calcium 12 hydroxy stearate does not have such problem and hence can be used up to 120°C. Its drop point (a temperature at which a grease melts) is about 145°C. Sodium soap greases tend to be fibrous relative to other types and can be used to about 120°C, the drop point ranging between 150°C to 230°C. They generally lack the oxidation resistance of lithium and clay greases. Lithium soaps (lithium 12-hydroxy stearate) are most versatile in use. The drop point is about 195°C and even after melting, when re-cooled, they usually return to a grease texture, although properties vary. They are resistant to water, oxidation and also mechanical working. Complex soap thickeners are nowadays much in use because of their high-drop point. Clay thickeners containing bentonite or hectorite clay are also used. They do not melt but have poor oxidation stability. Polymerized substituted ureas (polyureas) are also used in several cases. They have the drop point at about 260°C. Calcium soap greases are used in rolling element bearings where temperature extremes do not occur. Sodium soaps are generally used in plain journal and slider bearings and gears. Lithium soaps are used as multipurpose greases. Complex soaps are particularly used for high temperature applications.

Lubricating oil is the largest single component of grease (containing 65 to 95 per cent) and controls the frictional characteristics of greases. The overall performance of a grease is largely affected by the oil viscosity property, oxidation resistance, volatility, compatibility of oil, etc. Most lubricant greases used in industry have petroleum oils as their liquid base. The petroleum oil-based greases can be used up to 175°C depending on their thickener. The synthetic oil-based greases can be used at higher temperature. Silicon-based greases thickened with ammetine and silica can be used at temperatures up to 300°C.

1.5 VISCOSITY

The most important single property of a lubricant is its viscosity. The viscosity of a fluid is defined qualitatively as its resistance to flow. This resistance is primarily due to internal friction. Sir Isaac Newton was the first person to propose that a force is necessary to shear a fluid film. This force is a measure of internal friction of fluid and it resembles friction between two solid surfaces. In fluid film lubrication, load carrying capacity depends on the viscosity of the lubricant. A lubricant with extremely low viscosity cannot form a layer of fluid film between two sliding surfaces. Again, if the viscosity of a lubricant increases, the frictional resistance and heat generation in the bearing increases. Thus the choice of a lubricant with proper viscosity is an important consideration in bearing design.

Following Newton, for two surfaces separated by a fluid film of thickness h and having relative motion at a linear velocity u, the force per unit swept area (F/A) or shear stress (t) is proportional to the shear rate or the velocity gradient (du/dy) in the film (Fig. 10.1)
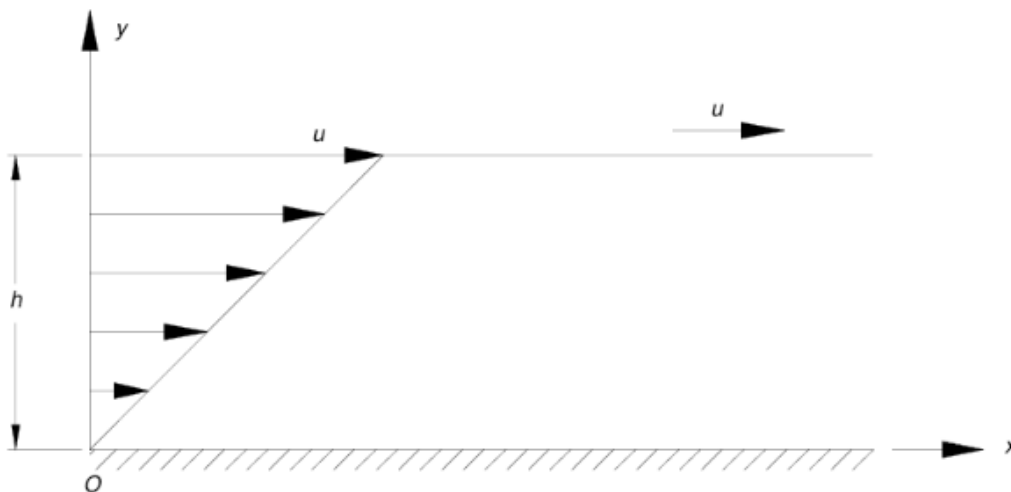
Fig. 10.1 Schematic representation of two parallel plates in relative motion with a velocity of u, separated by a fluid film of thickness h with a linear velocity gradient.

$$\tau = \frac{F}{A} = \eta \frac{du}{dy} \tag{10.1}$$

where η is known as absolute (dynamic) viscosity of the lubricant. If the velocity is a continuous function of the film thickness and there is no slip at the interface between the fluid film and the solid surfaces, then

$$\frac{du}{dy} = \frac{u}{h}$$

Thus Eq. (10.1) reduces to

$$\tau = \eta \frac{u}{h} \tag{10.2}$$

Any lubricant which obeys the above law is a Newtonian lubricant.

The unit of h is dynes-s/cm^2 (poise or P) or lb-s/in^2 (reyn) or N-s/m^2 (Pa.s). Conversion of units are 1 reyn = 68,750 P and 1 P = 0.1 Pa.s. To have a quantitative idea of absolute viscosity, water has a viscosity of the order of 1 centipoise (0.01 P) at room temperature and air h as a viscosity of 0.02 cp. The viscosity of most lubricant lies in the range of 2 to 400 cp. Another measure of viscosity is kinematic viscosity (n) equals h divided by density (r).
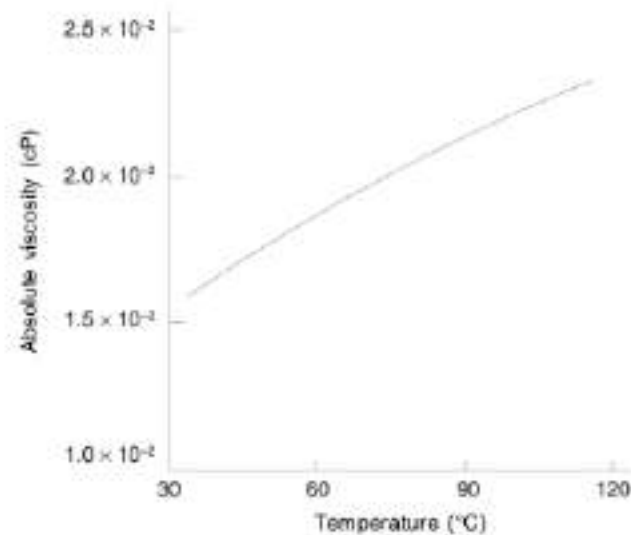
$$v = \frac{\eta}{\rho} \tag{10.3}$$

The unit for n is mm^2/s (centistoke or cSt).

Effect of Temperature, Pressure and Shear Rates on Viscosity

Viscosity of lubricant depends on temperature, pressure and, in many cases, shear strain rates. The viscosity of liquids is mainly due to intermolecular forces. If the temperature increases, the liquid starts expanding, the intermolecular distance increases and the intermolecular forces decrease which results in a fall of viscosity, for example, see
Fig. 10.2. A mathematical expression for viscosity-temperature relationship of a liquid may be given as

$$\tau = \frac{F}{A} = \eta \frac{du}{dy} \tag{10.1}$$

where η is known as absolute (dynamic) viscosity of the lubricant. If the velocity is a continuous function of the film thickness and there is no slip at the interface between the fluid film and the solid surfaces, then

$$\frac{du}{dy} = \frac{u}{h}$$

Thus Eq. (10.1) reduces to

$$\tau = \eta \frac{u}{h} \tag{10.2}$$

Any lubricant which obeys the above law is a Newtonian lubricant.

The unit of h is dynes-s/cm^2 (poise or P) or lb-s/in^2 (reyn) or N-s/m^2 (Pa.s). Conversion of units are 1 reyn = 68,750 P and 1 P = 0.1 Pa.s. To have a quantitative idea of absolute viscosity, water has a viscosity of the order of 1 centipoise (0.01 P) at room temperature and air h as a viscosity of 0.02 cp. The viscosity of most lubricant lies in the range of 2 to 400 cp. Another measure of viscosity is kinematic viscosity (n) equals h divided by density (r).

$$v = \frac{\eta}{\rho} \tag{10.3}$$

The unit for n is mm^2/s (centistoke or cSt).

Effect of Temperature, Pressure and Shear Rates on Viscosity

Viscosity of lubricant depends on temperature, pressure and, in many cases, shear strain rates. The viscosity of liquids is mainly due to intermolecular forces. If the temperature increases, the liquid starts expanding, the intermolecular distance increases and the intermolecular forces decrease which results in a fall of viscosity, for example, see
Fig. 10.2. A mathematical expression for viscosity-temperature relationship of a liquid may be given as

Fig. 10.3 Absolute viscosity of air as a function of temperature at atmospheric pressure.

The relationship between viscosity and temperature for mineral oils is expressed based on an arbitrary system of comparison using the viscosity index ($V.I.$). However, $V.I.$ relates the change in viscosity of the sample oil at two temperatures, 38°C and 100°C, to two arbitrary oils. At the time of its introduction, Pennsylvania oil and Gulf Coast oil were chosen as standards and given $V.I.$ of 100 and 0, respectively. This was because of the fact that the former showed the least variation of viscosity, while the latter suffered the greatest decrease of viscosity with temperature. The method of determining the $V.I.$ of an oil sample is shown in Fig. 10.4. The $V.I.$ can be calculated from the following relation

$$V.I. = \frac{\bar{L} - \bar{x}}{\bar{L} - \bar{H}} \times 100 \tag{10.5}$$

where

$\bar{L}$ = viscosity at 38°C of the sample oil

$\bar{H}$ = viscosity at 38°C of the oil with $V.I. = 0$

= viscosity at 38°C of the oil with $V.I. = 100$.
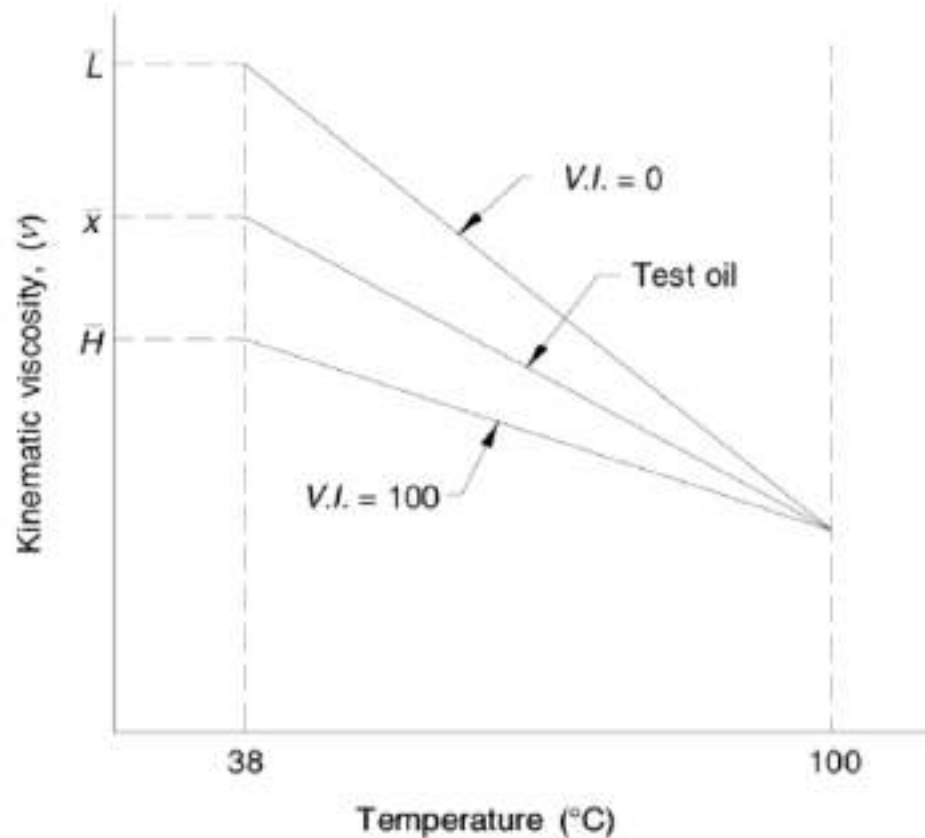
Fig. 10.4   Method of calculation of viscosity index (V.I.).

When the pressure of a liquid or gas is increased, the molecules come closer and intermolecular forces increase. As a result, viscosity changes. The viscosity of petroleum based mineral oils increases rapidly with an increase in pressure and by several orders of magnitude. Barus (1893) proposed the following relationship for liquids:

$$\eta = \eta_0 \exp(\alpha p) \tag{10.6}$$

where h and h_0 are the viscosities at pressure p (above ambient) and normal atmospheric pressure, respectively, a is pressure coefficient of viscosity in m^2/N (1/Pa) and p is normal pressure (Pa). The value of a at 38°C is found to be of the order of $2 \ \Box \ 10^{-8}$/Pa. Roelands (1966) proposed an expression for isothermal viscosity-pressure dependence which fits better the experimental data. The same can be written as

$$\log \eta + 1.200 = \left(\log \eta_0 + 1.200\right)\left(1 + \frac{p}{2000}\right)^{z_1} \tag{10.7}$$

where z_1 is a dimensionless constant known as viscosity-pressure index. Equations (10.4) and (10.6) can be combined as

$$\eta = \eta_0 \exp\left[\alpha p + \beta\left(\frac{1}{T} - \frac{1}{T_0}\right)\right] \tag{10.8}$$

Viscosity of fluids varies as a function of shear rate and the branch of study dealing with this is known as *fluid rheology*. A fluid that follows Eq. (10.2) is called a Newtonian fluid. In case of non-Newtonian fluids, viscosities vary with shear rate. Liquids with loose molecular structure such as water behave as Newtonian. Shear thinning (a phenomenon of thinning of fluid with increase in shear rate) occurs in case of so-called pseudo-plastic fluids. These fluids are generally composed of long molecules randomly oriented with no connecting structure. When shear stress is applied, the molecules tend to get aligned resulting in a reduction in viscosity. In dilatant fluids, shear thickening occurs, i.e., the fluid gets thickened with an increase in the shear stress. These fluids are usually suspensions having high-solid contact. For Bingham plastic fluids, some shear stress is required before the flow begins and these fluids usually possess a three-dimensional structure that can resist a certain amount of shear stress known as *yield stress*. Many greases act like Bingham fluids. When, for a material, viscosity depends on its previous shearing history, it is termed as thixotropic material. All solid and liquid polymers behave as thixotropic material to some extent. Figure 10.5 shows schematic curves for dependence of shear stress and viscosity on shear rate for different fluids.
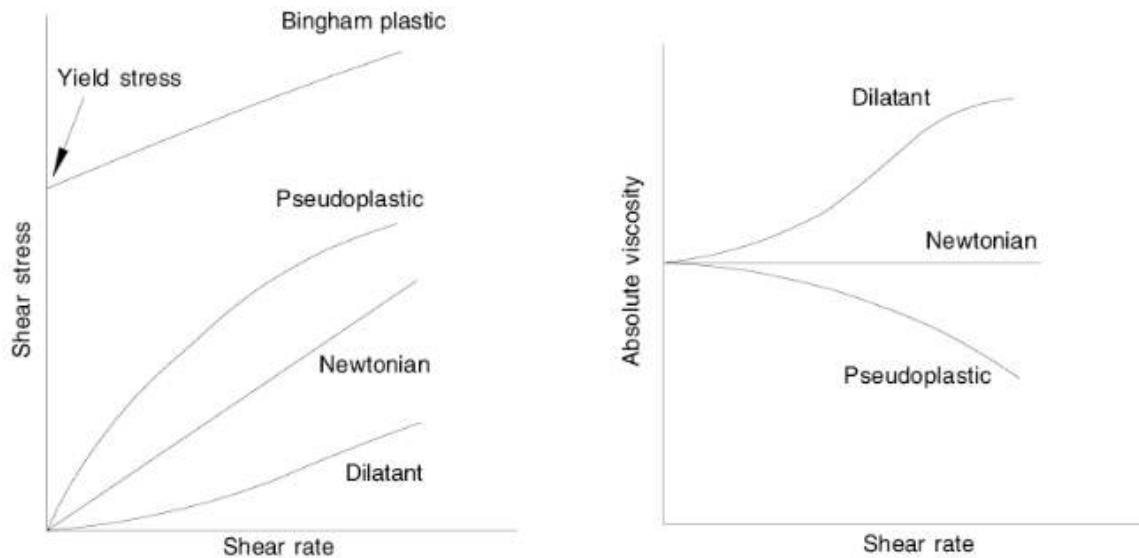
Fig. 10.5 Dependence of shear rate on shear stress and absolute viscosity for various fluids.

A large number of liquids become non-Newtonian at high-shear rates. Above a certain shear rate viscosity starts decreasing and the fluid behaves as non-Newtonian. This is known as *shear thinning*. A drop in viscosity also occurs due to thermal thinning as a result of viscous heating at high shear rates. At very high-shear rates, lubricant sometimes becomes plastic and can only support a constant stress known as the limiting shear strength, t_L (Fig. 10.6). This limiting shear strength is a function of temperature
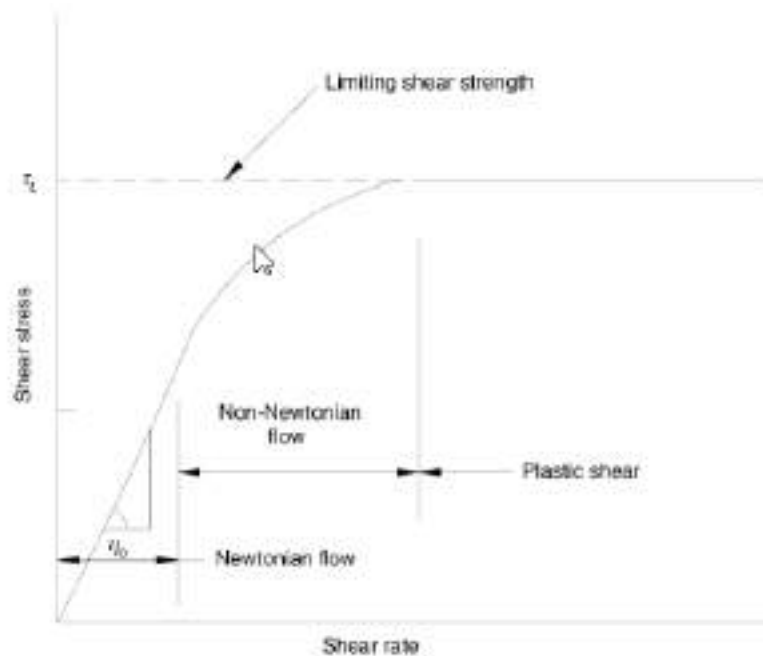
Fig. 10.6 Dependence of shear rate on shear stress for many liquid lubricants (non-Newtonian flow).

and pressure and increases at higher pressures and at lower temperatures. The value of shear rate at which the viscous plastic transition takes place increases with a decrease in the pressure and an increase in the temperature. Most liquid lubricants in non-conforming contacts such as in rolling element bearings behave as a plastic solid at high pressures (of the order of 0.1 to 1 GPa) and at relatively low-shear rates (of the order of 10 to 100/s). One of the rheological models which fits well in experimental data is due to Bair and Winer (1979) and may be given as

$$\tau = \tau_L \left[1 - \exp\left(-\frac{\eta_0 \dot{\gamma}}{\tau_L} \right) \right] \tag{10.9}$$

$$\tau_L = \tau_i + \xi p \tag{10.10}$$

where τ_0 is the shear strength at normal atmosphere and ξ is the limiting shear strength proportionality constant, i.e., $\partial\tau_L/\partial p$, $\dot{\gamma}$ is the shear rate and p is the pressure. The model suggests that for $\eta\,\dot{\gamma}/\tau_L > 5$, the material becomes a plastic solid and τ_L is linearly dependent on pressure.

Viscosity Measurement

The viscosity of lubricants can be measured by many methods based on different principles. Most commonly used instruments typically fall into four categories depending on geometry: capillary, rotational, falling sphere and efflux viscometers.

The capillary viscometer is based on measuring the rate at which a fluid flows through a small diameter tube and this takes the form of measuring the time taken to discharge a given quantity of liquid for an applied pressure difference and tube dimensions. In capillary viscometers a direct measurement of absolute viscosity is not possible and kinematic viscosity is measured. The kinematic viscosity is given as:

$n = c.t.$, where c is a constant for a given viscometer and t is the time required for a given volume of liquid to flow through the tube. By using some liquid of known viscosity and density, the time required for a given volume to flow through the capillary is determined and the constant for the instrument is found. The sketch of one such viscometer is shown in Fig. 10.7.

In rotational viscometers, the absolute viscosity of oil is measured. Three different types of rotational viscometers are used: cylindrical, cone-plate type and parallel-plate type. The cylindrical type is in the form of two concentric cylinders one of which rotates in the oil whose viscosity is to be measured. The viscosity measurements are made either by applying a fixed torque and measuring the speed of rotation, or by driving the rotating element at a constant speed and measuring the torque required. The cone-plate and parallel-plate rotational viscometers are the variations of the same technique. For viscosity measurements of non-Newtonian fluids, rotational viscometers involving shearing of the fluid are used. These instruments are usually calibrated with the fluids of known viscosity and the viscosities of test samples are taken from the calibration chart. Basic arrangement of cylindrical and cone-plate rotational viscometers are shown in Fig. 10.7.
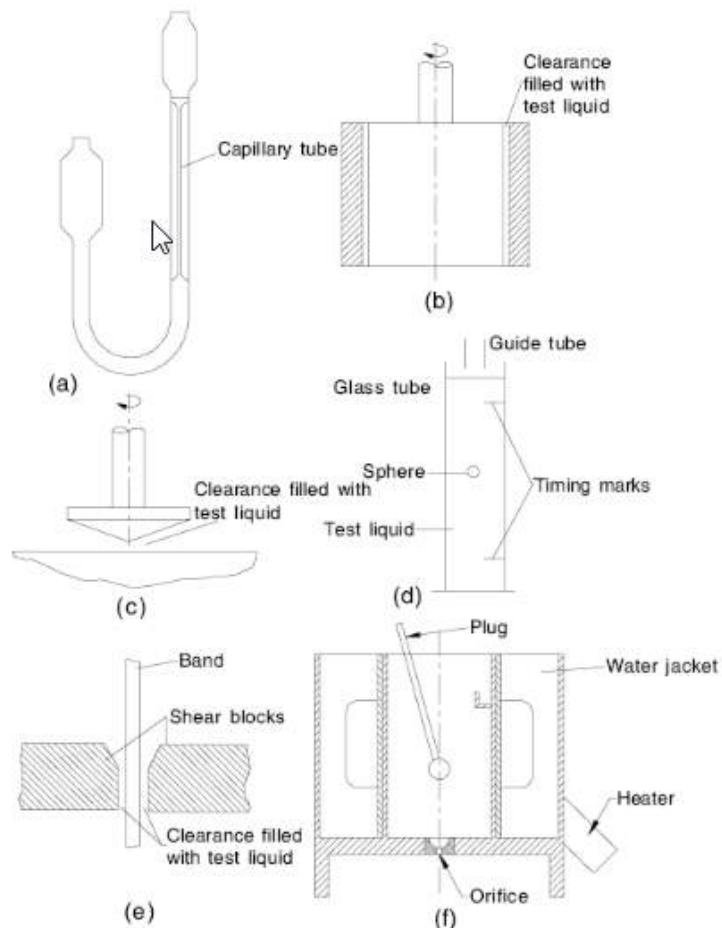
Fig. 10.7 Different viscometers: (a) u-tube viscometer (b) rotating-cylinder viscometer (c) cone and plate viscometer (d) falling-sphere viscometer (e) band viscometer (f) efflux viscometer.

In falling sphere viscometer [Fig. 10.7(d)], the time taken for a ball to fall through a measured height of fluid in a tube is measured. The time required is a measure of absolute viscosity. Other variations of this type are also available. In rolling-sphere viscometer, a ball rolls down an inclined tube filled with the test fluid. The falling coaxial cylinder viscometer consists of two coaxial cylinders with their axes vertical. The outer cylinder is clamped and the clearance space between the cylinders is filled with the test fluid. In operation, the inner cylinder is released and falls under gravity. Viscosity is determined from the speed of descent of the cylinder whose motion is opposed by the shear stresses induced in the test fluid. Another variety is the band viscometer

[Fig. 10.7(e)] where a thin band is located in a narrow gap between two parallel shear blocks filled with the test fluid. The band is released to fall under gravity, its motion being opposed by the shear stresses induced in the test fluid. Viscosity is determined from the speed of descent of the band. These types of instruments are useful for non-Newtonian measurements and for high-viscosity fluids.

In efflux viscometers, shown in Fig. 10.7(f) viscosity is measured by the time taken for a given volume of liquid to discharge under gravity through a short tube orifice placed in the base of the instrument. Three types of efflux viscometers are common: Redwood, Saybolt and Engler. The first one is commonly used in the U.K. while the second one is mainly used in Europe and the U.S.A. In all these three instruments, viscosities are quoted in terms of the efflux time, for example, Redwood sec, Saybolt sec or Engler sec. These measurements are then converted into kinematic viscosity by using conversion tables.

1.6   OTHER PROPERTIES

Relative Density

It is the density of the liquid divided by the density of water at the same condition of temperature and pressure. The density of liquid is required to calculate flow rates and for the conversion of kinematic viscosity to dynamic viscosity. Most mineral oils have relative densities in the range of 0.85 to 0.95 and the density in g/cc is very nearly numerically equal to the relative density. The change of density of lubricating oil due to working pressure existing in the bearings with fluid film lubrication is relatively small and may be neglected. In gas film lubrication, the variation of density with pressure must be considered.

Specific Heat and Thermal Conductivity

These are important properties if the oil acts as a coolant or heat transfer medium. For consideration of thermal equilibrium, these properties are needed. The specific
heat and thermal conductivity of most mineral oils are in the range of 0.45 to 0.5 and

$3 \square 10^{-4}$ Cal/cm-s-°C, respectively. Both these quantities do not change appreciably with change in temperature.

Acidity and Alkalinity

Traces of weak organic acids present in lubricating oils do not cause any harm. But acids formed by combustion or oxidation and introduced by contamination may cause harm. Acidity of oil is expressed in terms of neutralization number, which is defined as the weight of potassium hydroxide in milligrams required to neutralize one gram of oil.

In some specialized applications, alkalinity is introduced to give the oil special properties. Modern engine oils are made alkaline for the purpose of neutralizing fuel combustion products. In some cutting oils, alkalinity is introduced to protect ferrous metal from corrosion and to stabilize the emulsion. Alkalinity of oil is expressed in terms of base number, which is defined as the number of

milligrams of potassium hydroxide which are equivalent to the alkali present in one gram of oil.

Oxidation Stability

At room temperatures, the oxidation rate of mineral oils is fairly low but it is greatly accelerated at temperature above 90°C. The oxidation products vary but in general they consists of acidic compounds, sludge and lacquers. The insoluble products may clog oil holes, pipelines, filters and other elements. The soluble products may cause the oil to become corrosive and to increase in viscosity. Thus the oxidation has an influence on the life of oil as well as the lubricating system.

Flash Point

It is defined as the lowest temperature at which the vapour given off by oil, when heated in a standard apparatus, ignites momentarily on the application of a flame. It is a measure of the fire hazard and is also useful in determining whether oil has been contaminated. The knowledge of flash point of oils is particularly important when used in high pressure systems of aircraft or in forging presses where oil, leaking from a pipe, may come into contact with hot metal leading to fire hazards.

Foaming

Excessive foaming of oil due to churning may lead to inadequate lubrication and related problems. This is especially true for hydrostatic bearings where the pump used in the hydraulic line cannot deal efficiently with a frothy mixture.

Pour Point

It is defined as the temperature at which the oil just ceases to flow freely under the specified conditions. Thus it imposes a lower limit on the oil working temperature and determines the suitability of lubricants for low-temperature installations.

Demulsibility

This property is usually desired in oils, which may come into contact with water by leakage or by condensation. The demulsibility number of an oil can be found from a standard test which determines the time in seconds required for a known volume of oil to separate from an equal volume of condensed steam. Emulsifiable oils are used in metal cutting processes where the function of the emulsion is to cool the system rather than to lubricate.

Extreme-pressure Properties

A large number of machines are used for evaluating and comparing lubricating oils under extreme-pressure conditions. These machines involve highly loaded regions where sliding or combined sliding and rolling take place. A commonly used machine is a four-ball tester where parameters like friction, wear and seizure of load under extreme-pressure condition can be measured.

Questionnaires

1. What is the practical important of Tribology?

2. Write briefly about historical background of Tribology.

3. List the properties of Lubricants.

4. Explain the classification of lubricants and explain briefly.

5.Explain the effect of Temperature and Pressure on Viscocity.

Further Reading:

1. "Introduction to Tribology in bearings", B. C. Majumdar, Wheeler Publishing.

2. "Basic Lubrication Theory", A. Cameron, Ellis Hardwoods Ltd., UK.

Module 2

Contents:

- **Friction:** Origin, Friction Theories,
- Measurement Methods,
- Friction Of Metals And Non-Metals.
- **Wear:** Classification And Mechanisms Of Wear,
- Delamination Theory,
- Debris Analysis,
- Testing Methods And Standards.
- Related Case Studies.

Objectives

1. Introduction to friction and wear mechanisms
2. Measurement of friction and wear

2.1 ORIGIN OF FRICTION

History

Amontons considered that the surfaces were not completely smooth. The origin of friction was involved in the work done in lifting the load over the surface asperities or deforming them. Desaguliers was of the opinion that this surface roughness explanation was not true. He criticized this on the basis of observation that friction increased when the surfaces were made smoother. He attributed the frictional effects to areas of adhesion within the contact zone. This was criticized in the way that doubling the area of contact would double the amount of adhesion and hence double the friction force, but friction is practically independent of area. Coulomb also considered the possibility of adhesion as one of the significant contributors but stressed on the interlocking of the asperities of the two surfaces. He argued that under the tangential load, the surfaces moved apart against gravity due to sliding up the hills that accounted for the frictional work done. Leslie criticized the same with the argument that if friction is due to solely overcoming the gravity, then there can be no frictional effect on an average as there is no net increase in elevation of the moving body because of hills and

valleys on it. When one part slides up the hills, the other part somewhere slides down the valleys of roughness. Leonhard Euler also believed in the model of rigid interlocking of asperities. He introduced the use of symbol m for the coefficient of friction. He showed that if the asperities are assumed to be triangular and of slope q, then $m = \tan q$.

However, with the present understanding of the geometry of surfaces, the friction force is due to interactions between the opposing asperities of the two surfaces. In

these interactions energy is dissipated and is equal to the product of the friction force and the sliding velocity. The asperity interactions may be of two types: adhesion and deformation.

Adhesion

When two surfaces are loaded, the intimate contacts occur at the peaks of the asperities and the real area of contact is less than the nominal area. Thus the pressure at the points of real contact is very high and the outermost atoms of one surface are in close proximity to the similar atoms on the other surface. This is particularly appreciable when the surfaces are clean, free from oxides and other surface films and from absorbed gases. Thus the surfaces are seen to adhere to ultra-high vacuum (typically less than 10^{-8} Pa pressure). If one wishes to separate the surfaces, then sufficient force needs to be applied to pull or slide them apart. This is particularly significant in cases of soft and ductile materials like lead and indium where adhesion can readily be demonstrated under ordinary laboratory conditions. Under the high pressure at the asperity peaks, the surfaces, get 'cold welded' together. The junction so produced will be of comparable strength with respect to the parent materials and offers significant resistance to sliding.

Deformation

In absence of adhesion, frictional resistance may be attributed to the deformation of the material and its displacement during relative motion. The deformation interaction may be of two types: (a) microscopic interaction limited to the asperities only and

(b) macroscopic interaction involving ploughing of the bulk material. It may also include the ploughing of surfaces by wear debris trapped between them. The true ploughing grooves are often of the dimension with orders of magnitude greater than those of the asperities. Deformation and adhesion components are often not independent to each other. Their individual contribution to friction may or may not be significant. The magnitude of contribution depends on surface roughness, hardness of the materials and also on the shape, size and hardness of the wear particles trapped between them. As a result, the friction coefficient varies widely in magnitude depending on materials and conditions.

2.2 FRICTION THEORIES

Bowden and Tabor's Simple Adhesion Theory

It has already been discussed that when two surfaces are loaded, the intimate contacts occur at the peaks of the asperities and the real area of contact is very less compared to the nominal area. The

pressure at the points of real contact is so high that the asperity tips of the softer material deform plastically and the plastic flow causes the total contact area to grow. This growth of contact area takes place by two means: (a) one by growth of individual contact spots and (b) by initiation of new contacts. The process continues until the total real area of contact is sufficient to support the load elastically. Then, for an elastic–plastic material, the normal load W may be expressed as

$$W = A \cdot p_0 \tag{5.2}$$

where A is the real area of contact and p_0 is the yield pressure of softer material and it is very close to the hardness, H. Hence

$$W = A \cdot H \tag{5.3}$$

As the plastic deformation becomes severe, the asperity junctions get 'cold welded' and strong 'adhesive bonds' are formed. The force required to cause shear failure of the asperity junctions, i.e., the friction force due to adhesion, F_{adh}, is then

$$F_{adh} = A \cdot s \tag{5.4}$$

where s is the shear strength of the softer material. Thus the coefficient of friction due to adhesion may be written as

$$\mu_{adh} = \frac{F_{adh}}{W} = \frac{s}{H} \tag{5.5}$$

For most materials, this ratio of s/H is almost constant. Typical value for most metals is 0.2. Hence this theory predicts a value of friction coefficient as 0.2.

This theory looks very attractive because of its simplicity, but suffers from several inadequacies. They are as follows:

(a) The first inadequacy relates to the fact that the friction coefficient in this model does depend only on the properties of the softer material. It means one can expect the same value of friction coefficient for a particular material sliding against any other harder material. But it is not true as experiments show that the value of friction coefficient does depend on the pair of material concerned.

(b) Under normal atmospheric conditions, the actual values of friction coefficient for metal pairs are found normally to be in the order of 0.5 rather than 0.2 as predicted by the theory.

(c) Friction coefficients are seen to be much higher than that predicted by this theory, even more than unity, in cases of many materials under contaminant free sliding conditions as in ultra-high vacuum.

In the simple adhesion theory of friction, the material is assumed to have a constant value of flow

stress. But almost all metals strain-harden to some extent and this will tend to increase the value of s relative to that of H. Work hardening will, therefore, tend to increase m_{adh}.

Modified Adhesion Theory: Junction Growth

The drawbacks of simple adhesion theory led to the development of modified adhesion theory. Professors Bowden and Tabor re-examined their earlier theory and modified considering the combined effect of the normal and shear stresses. This is unlike the earlier case, where the effects of the normal and tangential loads were considered separately. It was considered that the normal load determined the real area of contact, and to shear over this area, tangential force was needed. But the very high friction coefficients observed in the case of clean metals point to the fact that the true contact area must be much greater than that predicted by the normal load alone.

Let us consider an element subjected to uni-axial compression by a normal stress p_0. We can assume it to be on the point of yielding. If a tangential stress is now applied to it, it experiences an additional shear stress s. For the material to remain at the point of yielding, the normal stress on the element must reduce to some value p_1. If the normal load remains constant, then the area of contact must grow. This phenomenon is thus known as *junction growth*. For Tresca's criterion, the relationship between p_1, s and p_0 is given by

$$p_1^2 + 4s^2 = p_0^2 \qquad (5.6)$$

For the von Mises yield criterion,

$$p_1^2 + 3s^2 = p_0^2 \qquad (5.7)$$

Both the relationships lead to the same qualitative conclusions though they differ in the coefficient of s^2. Now if we use $p_1 = W/A$ and $s = F/A$, F being the tangential load, then Eq. (5.6) leads to

$$W^2 + 4F^2 = A^2 p_0^2 \qquad (5.8)$$

In any typical deadweight sliding experiment, W is constant, while p_0 is a property of the material. The real area of contact A will thus increase with the increasing tangential force and hence the ratio F/W, the instantaneous value of coefficient of friction will also increase.

Theoretically, the growth process could continue until the entire area of the specimen is in contact, but in most practical cases, the ductility of the material and the presence of weak interfacial films limit it. The effect of weak interface can be modelled assuming that it will fail at some shear stress value s_i, less than the shear strength of the bulk material. Then the maximum tangential force is given by

$$F_{\text{max}} = A \cdot s_i \qquad (5.9)$$

If the shear yield stress of the bulk material is s_0, then from Tresca yield criterion $p_0 = 2s_0$. The coefficient of friction can then be derived as

$$\mu = \frac{F_{\text{max}}}{W} = \frac{1}{2\sqrt{(s_0/s_i)^2 - 1}} \qquad (5.10)$$

when the interface has the same shear strength, as that of the bulk material m becomes infinite, as junction growth is unlimited. When interface is weak, m is finite and drops rapidly as the ratio s_i/s_0 falls. The dependence of m on this shear strength ratio s_i/s_0 is shown in Fig. 5.4. The figure shows that for an interfacial strength one-tenth of the bulk value, $m = 0.05$. For an interface with half the bulk strength, m falls to about 0.3. Thus weak interfacial films lead to a very limited junction growth and reduce the value of m. If a film of material of low shear strength can be incorporated between the two surfaces, then the coefficient of friction can be lowered.
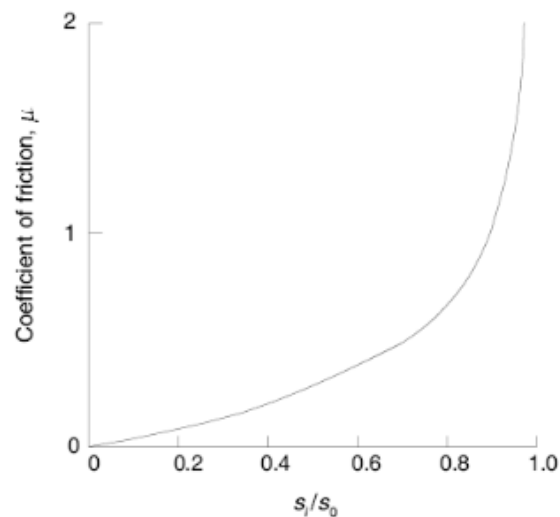
Fig. 5.4 Variation of coefficient of friction, μ with the ratio between the shear strength of the interface and that of the bulk material.

Deformation Theory: Ploughing

In cases where the adhesion term is small, ploughing becomes a dominant component of friction. If one of the surfaces in sliding contact is harder than the other, the asperities of the harder surface may penetrate and plough into the softer surface and produce grooves when shear strength is exceeded.

Ploughing may also occur as a result of impacted or entrapped wear particles. Interaction of two rough surfaces may result in mechanical inter-locking on a micro- or macro-scale, which, in turn, results in ploughing of one of the surfaces during sliding. Ploughing not only increases friction, but also creates wear particles, which, in turn, increase subsequent friction and wear.

Ploughing component of friction may be calculated using model rigid asperities or entrapped wear particles. Four such model asperities are considered: (a) conical, (b) spherical, (c) upright cylindrical and (d) transverse cylindrical. During sliding only the front surface of the asperity comes into contact with the softer body. Therefore, the normal load W is supported by the horizontal projection of the asperity contact area (A_H) and the friction force (F) is supported by the vertical projection of the asperity contact area (A_V). Considering the yield pressure of the solid as p_0 and the yielding of the body to be isotropic

$$W = p_0 \cdot A_H \tag{5.11}$$

$$F = p_0 \cdot A_V \tag{5.12}$$

Thus, the coefficient of friction due to ploughing is given by

$$\mu_p = \frac{F}{W} = \frac{A_H}{A_V} \tag{5.13}$$

Figure 5.5(a) shows a hard conical asperity sliding on a softer material. For this case

$$A_V = \frac{1}{2}(2rd), A_H = \frac{1}{2}\pi r^2$$

Therefore,

$$\mu_p = \frac{A_V}{A_H} = \frac{\frac{1}{2}(2rd)}{\frac{1}{2}\pi r^2} = \frac{2}{\pi}\left(\frac{d}{r}\right) = \frac{2}{\pi}\cot\theta \tag{5.14}$$

where q is the apex semi-angle of the conical asperity. For most engineering surfaces, this semi-apex angle is very large (nearer to 90°) and the ploughing component of friction is accordingly small. For example, for a conical asperity with an apex angle of 170° on a very rough surface, the ploughing component of friction is only 0.056. This is a low value. It is so because in the analysis, the piling up of the material ahead of the sliding asperity is neglected. For abrasive material and impacted wear particles, the apex angle may be small and correspondingly the value of the ploughing component of friction may be large.
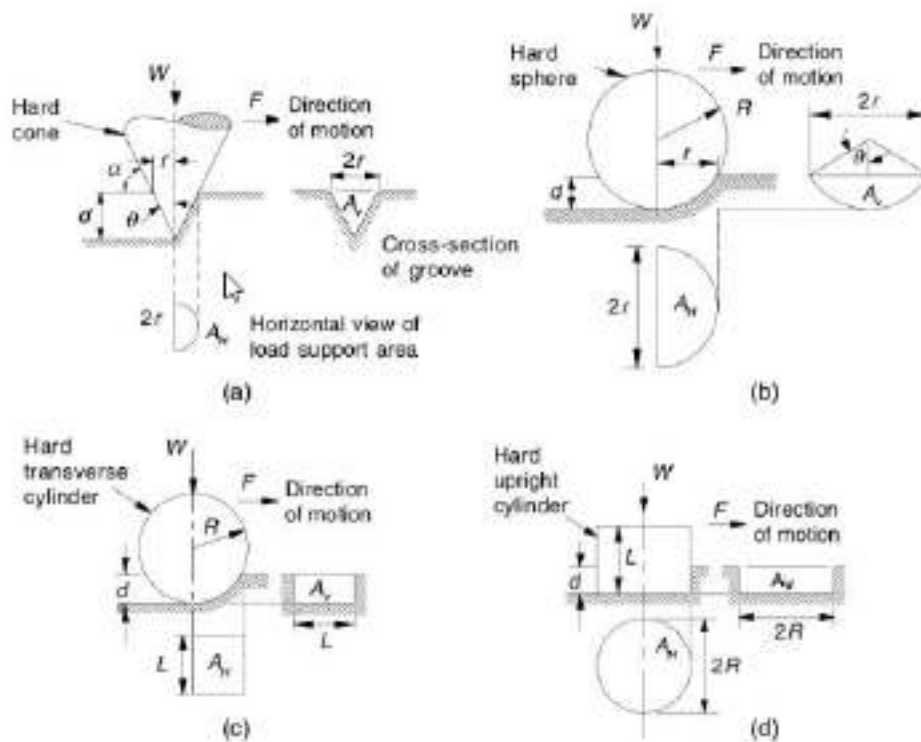
Fig. 5.5 Schematic representation of (a) hard cone (b) hard sphere (c) hard transverse cylinder and (d) hard upright cylinder sliding on a softer material.

For a spherical asperity of radius R in contact with a softer material [(Fig. 5.5(b)]

$$A_H = \frac{1}{2}\pi r^2 \quad \text{and} \quad A_V = \frac{1}{2}R^2(2\theta - \sin 2\theta)$$

But $\sin 2\theta = 2\theta - \frac{(2\theta)^3}{3!} + \cdots$

For small θ,

$$A_V = \frac{1}{2}R^2\left(2\theta - 2\theta + \frac{8\theta^3}{3!}\right) = \frac{2}{3}R^2\theta^3$$

Again, $\sin\theta = (r/R) = \theta$ for small θ. Therefore,

$$A_V = \frac{2}{3}\frac{r^3}{R}$$

2.3 MEASUREMENT METHODS

The basic principle of any friction-measuring instrument is to place two specimens together under a specified normal load and in relative motion while the tangential force resisting motion is measured. Many methods of varying specimen geometry, loading condition and resisting force measurement are available. Different researchers use many ingenious set-ups to investigate different specific cases.

5.2.1 Inclined Plane Rig

The simplest arrangement is the inclined plane test shown in Fig. 5.1. A specimen is placed on a flat plane whose inclination with the horizontal is gradually increased until the specimen on it starts sliding. If the inclination at this moment be q, then $m_S = \tan q$. Obviously, this method is incapable of evaluating friction in continuous sliding.
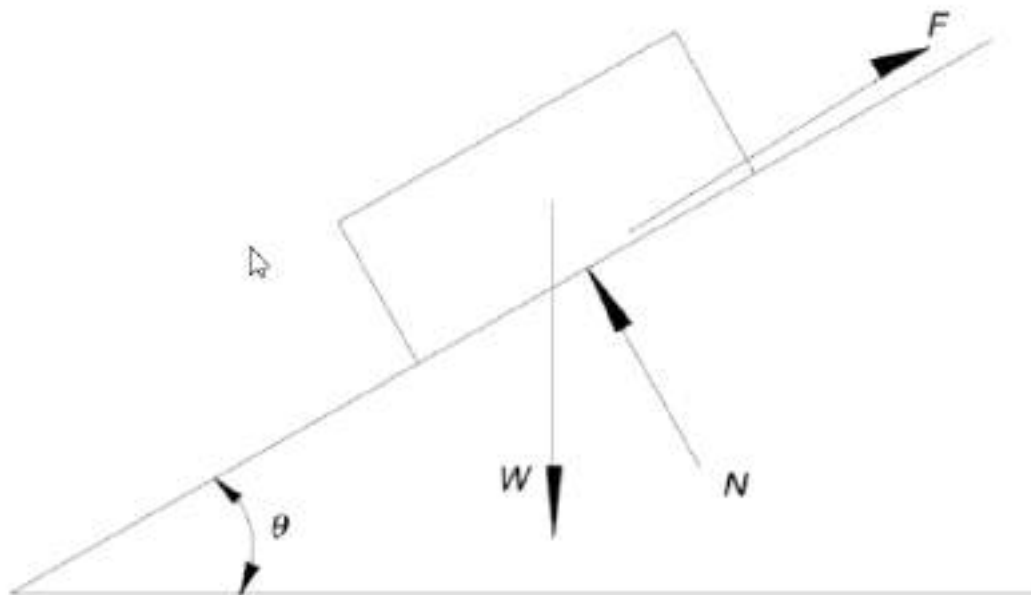
Fig. 5.1   Measuring friction by an inclined plane test rig.

Pin-on-disk Rig

In continuous sliding cases, the rig based on pin-on-disk configuration (Fig. 5.2) is used. The pin is held stationary under a normal load while the disk is made to rotate. The loading can be provided by simple dead weight or by spring loading or hydraulic or pneumatic pressure. The friction force is measured with the help of the calibrated tangential movement of a capacitive or inductive transducer mounted on the stationary specimen. For a multiple-pass arrangement, the pin is held at a constant radial distance from the centre of the disk, but in a single-pass arrangement it is moved radially during the experiment. Other standard arrangements such as pin-on-cylinder, crossed cylinders, reciprocating arrangement have been shown in Fig. 5.3.
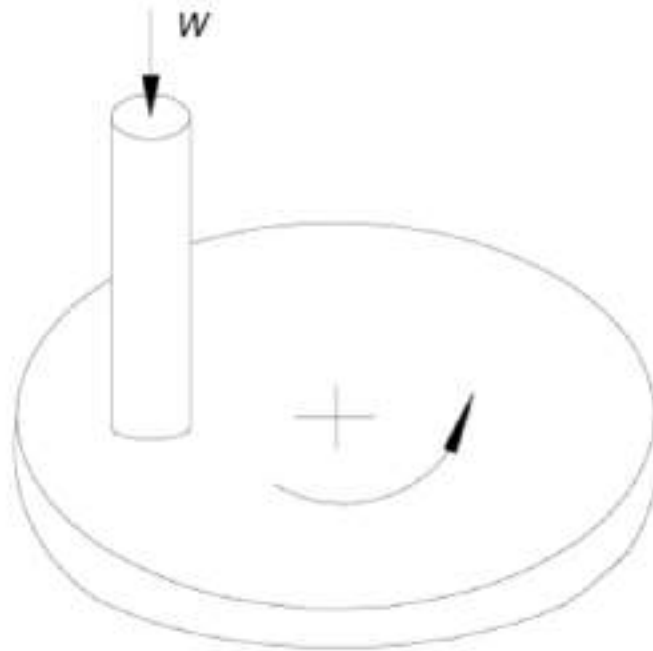
Fig. 5.2 Pin-on-disk friction measuring device.
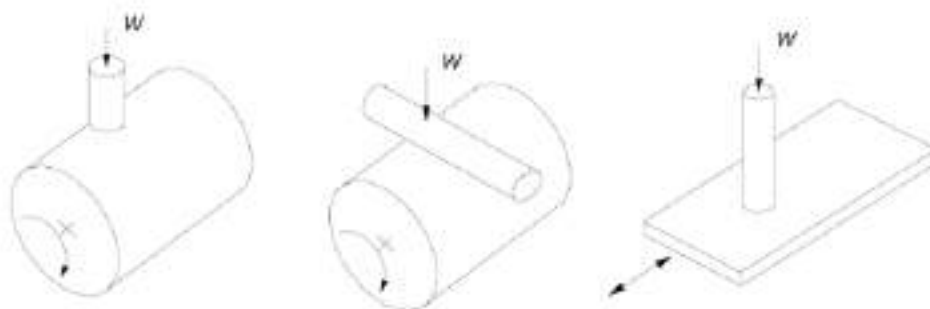
Fig. 5.3 Friction-measuring devices: (a) pin-on-cylinder (b) crossed cylinders (c) reciprocating rig

Conformal and Non-conformal Geometry Rig

The test rigs can be classified into two groups depending on the test geometry: conformal and non-conformal geometry test. In conformal geometry test, the profiles of the two contacting surfaces are matched carefully before the experiment is started. In this case, the contact pressure is moderate and normally held constant throughout the experiment. The test may then be used to simulate the situations such as brakes, thrust bearings, plane bearings, face seals, clutches, etc. On the other hand, in non-conformal geometry test (with spherically profiled pin) contact pressure is initially high because on first loading contact is made at a single point, and with time, pressure reduces due to development of small wear scars. This can be used to simulate the heavily loaded contacts such as gear teeth or to provide accelerated tests of friction and wear of a number of candidate material pairs for specified applications.

5.2.4 Environment Control

For accurate investigation the friction test must be carried out in an enclosed environment having simulated environmental conditions. Different friction pairs are susceptible to the presence of liquid lubricants, water vapour, gases, etc. If pin-on-disk tests are carried out in the presence of liquid lubricants, the results vary due to poorly controlled hydrodynamic conditions at the interface. Sometimes the small deformations of the rig caused by the thermal loading or pressure loading may give rise to experimental scatter. So many other forms of test rigs have been developed for specific applications involving different environmental conditions. For example, space environ-ments are simulated by the use of high-vacuum condition where the entire test rig is installed inside the vacuum chamber.

2.4 FRICTION OF METALS

The coefficient of friction of a particular material depends on the mating material, surface roughness and operating conditions. Thus the usefulness of coefficient of friction values from any published literature lies more in their relative magnitudes than in their absolute values. Table 5.1 lists some representative values of the coefficient of friction of metals and alloys taken from the literature.

**Table 5.1** Typical Values of μ_s and μ_k of Unlubricated Metals and Alloys

Material	μ_s		μ_k	
	Self-mated	On mild steel	Self-mated	On mild steel
Au, Pt	2	–	1–1.5	0.4–0.5
Ag	0.8–1	0.5	0.8–1.2	0.3–0.5
In, Pb, Sn	1	1.2–2	0.8–2	0.5–0.8
Al	0.8–1.2	0.5	0.8–1.2	0.5–0.6
Cr	0.4	0.5	0.5–0.6	0.4–0.5
Cu	0.7–1.4	0.8	0.8–1.2	0.6–0.7
Fe	0.5–0.8	0.5–0.8	0.8–1.5	0.8–1.5
Mg, Mo	0.5	0.4	0.5–0.6	0.4–0.6
Ni	–	–	0.7–0.9	0.6–0.9
Lead-based white metal	–	0.5	–	0.25–0.6
Leaded brass	–	0.2	–	0.2–0.4
Leaded bronze	–	–	–	0.2–0.4
Gray cast-iron	–	0.4	0.8–1	0.3–0.5
Mild steel	–	0.8	0.7–0.9	–

When metal surfaces are cleaned in high vacuum and placed in contact, strong adhesion is observed and consequently high friction is exhibited, typically 2 to 10 or even more for the value of coefficient of friction. Strong metallic bonds form across the interface and when the surfaces are pulled apart, metal gets transferred from one body to other. Gross seizure frequently occurs and sliding friction under ultra-high vacuum conditions occurs in space applications. With no interfacial contamination, the extent of junction growth is limited only by the ductility of the material. Gold is ductile and forms no oxide film in the air. Thus a considerable amount of junction growth in gold contact leads to high frictional value for gold.

Most metals oxidize typically in the air forming oxide film between 1 and 10 mm thick within a few minutes exposure of an atomically clean surface. These films play a crucial role in friction characteristics. Fig. 5.8 shows the effect of oxygen on the sliding friction of pure iron. The effect of an oxide film in reducing friction can be destroyed, if the film is penetrated during sliding with the application of increased normal load. This feature is shown in Fig. 5.9. At low-normal loads, the oxide films separate the two metals and the coefficient of friction is low because the oxide has low-shear strength and its low-ductility limits junction growth. At higher loads, the surface films deform and metallic contact occurs leading to high coefficient of friction. For some very soft and ductile metals like tin and indium, metallic contact between the surfaces occurs even at light loads and

consequently coefficient of friction is high without any marked change with load. For chromium, a thin but very strong oxide film is formed and no metallic contact occurs over a wide range of load leading to a low-constant friction coefficient. In general, the coefficient of friction for alloys tends to be lower than that of its pure elements. Binary alloys of Co and Cr with more than 10% Cr show excellent resistance to oxidation and corrosion. To improve friction and wear properties, tungsten and molybdenum are added. Lead-based white metals, brass, bronze and grey cast-iron exhibit low coefficient of friction because these contain phases that form films of low- shear strength. In grey cast-iron, a low-shear strength film is formed by the graphite constituent, while in lead-based alloys, a thin film of lead is formed during sliding. These alloys are commonly used in bearing and seal materials.

The friction coefficient of metals and alloys is affected by a number of operating parameters. As stated earlier, surface cleanliness plays a vital role in modifying friction behaviour. Apart from this, sliding velocity, contact pressure, temperature, relative humidity and gaseous environment affect friction behaviour to a great extent. High sliding velocities or high-contact pressures result in surface frictional heating which, in turn, results in the formation of a thin molten layer at asperity contacts in case of low melting points metals. This leads to reduction in shear strength and drop in friction coefficient, as shown in Fig. 5.10.
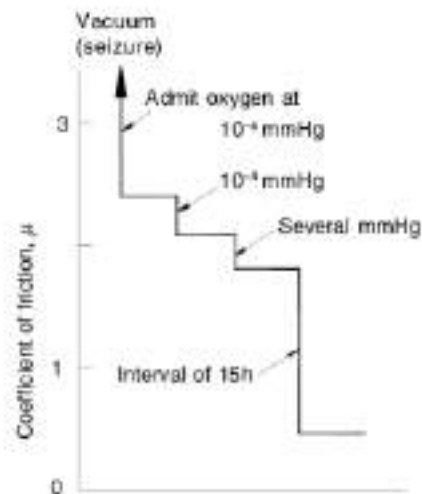
Fig. 5.8 The effect of oxygen on the friction of pure iron in vacuum, the value of μ is very high and falls as the oxygen concentration is increased [Buckley, 1981].
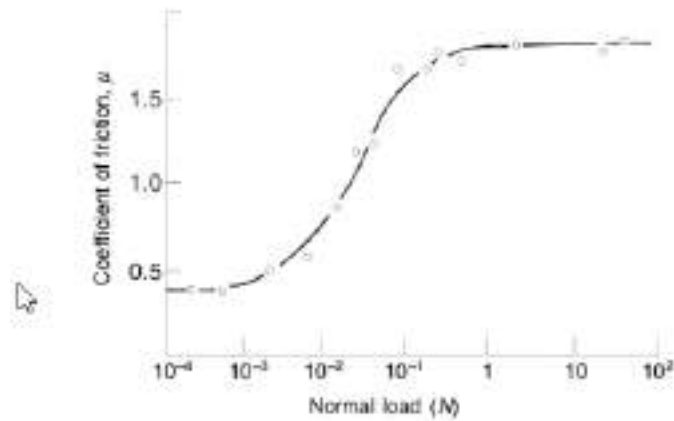
Fig. 5.9 The variation of the coefficient of friction with applied normal load for copper sliding against copper in air, unlubricated [Whitehead, 1950].
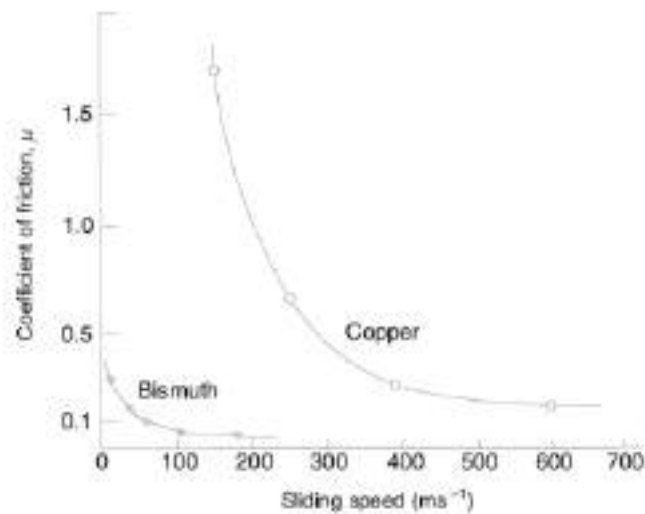
Fig. 5.10 The variation of coefficient of friction with sliding speed for pure bismuth and copper sliding against themselves [Bowden and Tabor, 1964].

Solid-state phase transformation also influences friction. Figure 5.11 shows the variation of the friction of cobalt with temperature. Cobalt exhibits a phase transformation at 417°C from a hexagonal close-packed structure with limited slip ductility to a cubic-packed structure, which is fully ductile. This phase transformation results in a peak in friction at about 500°C. Drop in friction above 550°C may be attributed to an increase in oxide thickness and also to a change in oxide species from CoO to Co_3O_4
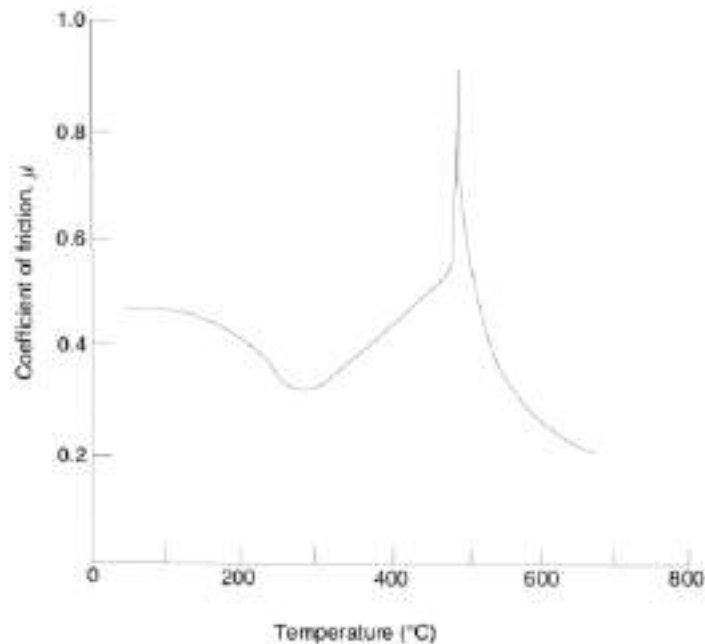
Fig. 5.11 Coefficient of friction as a function of temperature for cobalt sliding on stainless steel at a normal load of 5 N and sliding velocity of 25 mm/s [Rabinowicz, 1995].

2.5 FRICTION OF NON-METALLIC MATERIALS

5.7.1 Ceramics

Ceramics combine low density with excellent mechanical properties (e.g., high strength, stiffness, hardness) up to high temperatures. Engineering ceramics include silicon nitride (Si_3N_4), silicon carbide (SiC), alumina (Al_2O_3) and zirconia (ZrO_2). Ceramic pairs are commonly used in extreme environmental applications, such as high loads, high speeds, high temperatures and corrosive

environments. The mechanical behaviour of ceramics differs from that of metals due to different nature of inter-atomic forces— covalent or ionic bonding in ceramics compared to metallic bonding in metals. Because of the different nature of bonds, ceramics show limited plastic flow at room temperature and correspondingly much less ductility than metals. Although adhesive forces are present between ceramic pairs, low-real area of contact leads to relatively low friction in comparison to metallic pairs in presence of oxide films. In clean environments, friction coefficients of ceramic couples do not reach the high values as observed in clean metals in high vacuum. Friction coefficient of ceramics decreases with an increase in fracture toughness. The occurrence of fracture leads to higher friction as it provides an additional mechanism for the dissipation of energy at the sliding contact. Figure 5.12 shows the coefficient of friction as a function of fracture toughness for a sharp-diamond tip on SiC, Si_3N_4, Al_2O_3 and ZrO_2 disks produced under various hot pressing conditions.

Fracture is readily produced in concentrated contacts, e.g., a sharp–hard pin sliding against a flat. Figure 5.13 shows results from experiments where a diamond cone slided over a single crystal of silicon carbide. At low loads, no fracture occurred with plastic grooving and friction was low. With increase in load, fracture occurred leading to higher friction. The role of normal load, sliding speed, temperature and test duration on friction of ceramics may be interpreted in terms of changes in the tribo-chemical surface films and also the extent of fracture in the contact zone. Load and speed affect the temperature at the interface. Figure 5.14 shows the effect of sliding speed on friction coefficient of silicon carbide and silicon nitride in self-mated sliding. A similar behaviour has been reported in alumina and zirconia also. With sliding speed, the interface temperature increases and this enhances the tribological film formation on the sliding surfaces leading to a decrease in friction. Figure 5.15 shows the variation of coefficient of friction as a function of the temperature for alumina and zirconia, sliding in self-mated pairs in the air. The removal of absorbed water from the interface results in the initial rise in friction with temperature.
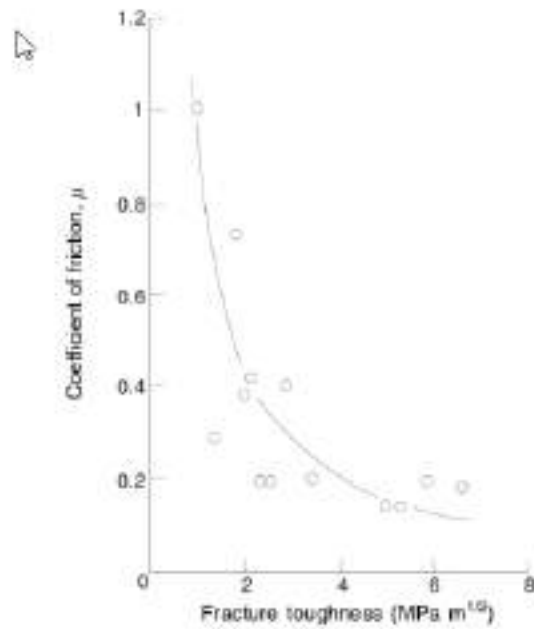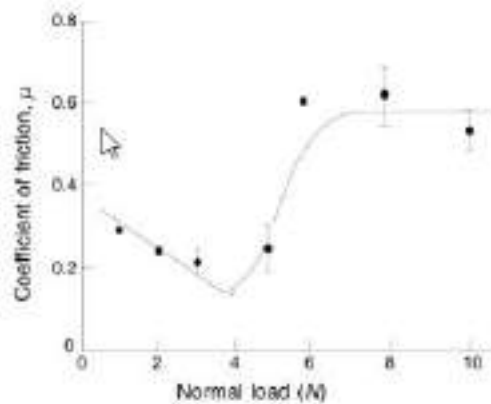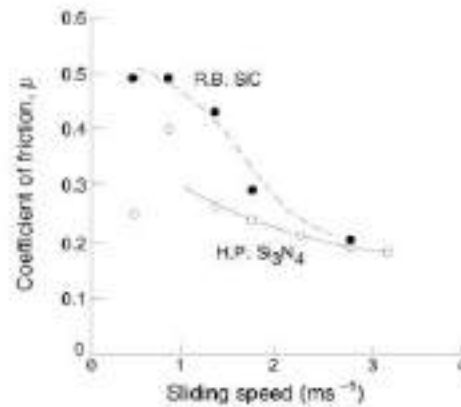
Fig. 5.12 Coefficient of friction as a function of fracture toughness for a sharp diamond pin (5 μm radius) on disks made of SiC, Si$_3$N$_4$, Al$_2$O$_3$ and ZrO$_2$ produced under various hot pressing processes [Ishigaki, Kawaguchi, Iwasa and Toibana, 1985].
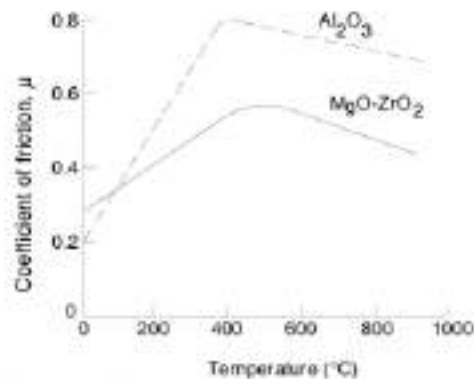
Fig. 5.13 Variation of coefficient of friction with normal load for a 60° diamond cone sliding over the (0001) face of a silicon carbide single crystal. The increase for loads above – 4 N is associated with fracture along the sliding path [Adewoye and Page, 1981].

Fig. 5.14 Variation of coefficient of friction with sliding speed for reaction-bonded silicon carbide and hot-pressed silicon nitride samples sliding in self-mated couples in the air [Cranmer, 1985].
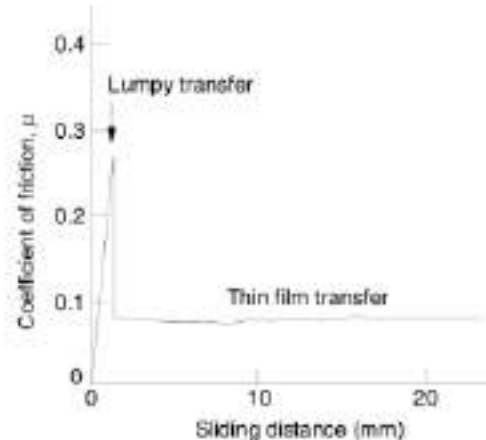
Fig. 5.15 Variation of coefficient of friction with temperature for magnesia-partially stabilized zirconia and alumina sliding against themselves [Hannink, 1984].

Polymers

Polymers include plastics and elastomers. The coefficient of the friction of polymers ranges between 0.15 and 0.6, in general, with the only exception of polytetrafluoro-ethylene (PTFE) which has typically a very low coefficient of friction 0.05. Thus polymers exhibit, in general, low friction in comparison to metals and ceramics, but very compliant with low elastic modulus values, typically one-tenth of metals or even less. Commonly used plastics are PTFE, high-density polyethylene (HDPE), polyphenylene sulfide (PPS), phamide (Nylon), polyimide, acetal, etc. Commonly used elastomers include natural and synthetic rubber, styrene butadiene rubber (SBR), silicon rubber and butadiene acrylonitrile rubber. These polymers belong to the category of self-lubricating solids. They flow readily at moderate pressures and temperatures. Since polymers lack in rigidity and strength, polymer composites are used to provide a combination of mechanical strength with low friction and wear. Carbon, graphite and glass are commonly used as fillers in polymer composites.

When plastics slide against hard metal surfaces, transfer film of plastic is formed on the mating surface and this governs the friction and wear behaviour. Sliding tends to occur at the interface between the bulk polymer and the transfer film, leading to low-wear rates. The coefficient of friction for initial sliding on a clean hard substrate is not particularly low (typically $m = 0.2$ to 0.3) and the transfer film is of the order of micrometers thick. As sliding continues, the coefficient of friction drops to a much lower value. The transfer film becomes much thinner and contains molecular chains strongly oriented parallel to the sliding direction. Such behaviour for HDPE sliding on glass is illustrated in Fig. 5.16. PTFE also shows similar behaviour. Because of lower friction behaviour, HDPE and PTFE have important applications as solid lubricants and bearing materials.

Fig. 5.16 Variation of coefficient of friction with sliding distance for high-density polyethylene (HDPE) sliding against glass [Pooley and Tabor, 1972].

The friction of polymers differs fundamentally from that of metals in one important respect that contact between polymers is often predominantly elastic. The mechanical property ratio (E/H) along with surface roughness determines the extent of plasticity in the contact region. For metals, the value of E/H is typically 100 or greater, whereas for polymers it is of the order of 10. The plasticity index for a polymer is of the order of one-tenth of that of a metal and the contact is thus almost completely elastic, except against very rough surfaces. The friction of polymers is also governed by the strong time-dependent mechanical properties of polymers (visco-elasticity). The main sources of friction are adhesion, deformation and elastic hysteresis. According to the analysis of adhesion, the coefficient of friction is affected by surface roughness and normal load. Fig. 5.17 presents the coefficients of friction values for rough and smooth polymethylmethacrylate (PMMA) sliding on them as a function of load. For smooth PMMA, the coefficient of friction decreases with an increase in a normal load while for rough PMMA, friction coefficient remains constant at low loads and decreases with a load at high loads. At high loads, elastic deformation at the asperities is so great that the individual asperities on the contacting surfaces are totally deformed and the contact region tends to a large single asperity contact. In such a case

$$m \propto W^{-1/3}$$
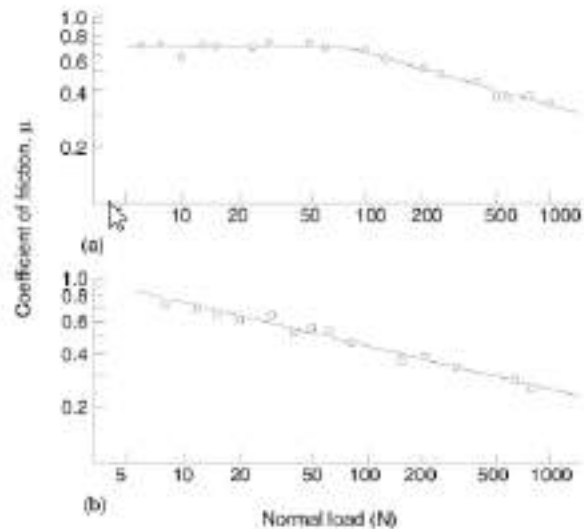
Fig. 5.17 Variation of coefficient of friction with normal load for sliding of crossed cylinders of polymethylmethacrylate (PMMA) with different surface roughness: (a) lathe turned and (b) smooth polished [Archard, 1957].

The adhesion responsible for polymer friction results mainly from the weak bonding forces (e.g., hydrogen bonding and Van der Waals forces), which are also responsible for the cohesion among the polymer chains themselves in the bulk of the material. Polar polymers tend to show strong adhesion because of high surface energy. The junctions formed by adhesion show many similarities to those responsible for the friction of metals. Very limited junction growth occurs in polymers and this accounts for the fact that m for polymers never reach the high values as exhibited by metals.

2.6 INTRODUCTION

The removal of material from one or both of two solid surfaces in relative motion (sliding, rolling or impact) is termed as *wear*. Surface damage due to material displacement with no net change in volume or weight is also called wear. It occurs as a natural consequence and mostly through surface interactions at asperities. It is a system response and it is not a material property. Interface wear is strongly dominated by operating conditions. Wear can be either desirable or undesirable. Desirable cases of wear include machining, polishing, shearing and writing with a pencil whereas undesirable cases include almost all machine applications such as bearings, gears, cams and seals. Sometimes it is erroneously assumed that high friction means high wear rates. But this is not true. Interfaces with solid lubricants and polymers show relatively low friction but high wear, while ceramics show moderate friction with extremely low wear. In some isolated cases, friction and wear may be correlated. But, in general, friction and wear are two distinct system responses.

2.7 TYPES OF WEAR

Wear takes place either by a mechanical process or by a chemical process or by combination of both and is generally accelerated by thermal processes (frictional heating). In different literatures, wear is classified into a number of categories based on the mechanism and severity of material removal. However, it can be broadly classified into four main forms:

(a) Adhesive wear

(b) Abrasive wear

(c) Corrosive wear

(d) Fatigue wear.

Besides these, a few marginal processes are often classified as minor forms of wear.

2.8 ADHESIVE WEAR

Adhesive wear takes place when two nominally flat solid surfaces are in sliding contact. At the interface asperities, contact and bonding take place due to adhesion. These contacts get sheared during sliding, resulting in detachment of a fragment from one surface and its attachment to the other surface or formation of loose wear particles. Some get fractured by a fatigue process during repeated loading and unloading process resulting in the formation of loose wear particles.

Several mechanisms exist for the formation of wear particles. According to Archard's theory of sliding wear, shearing of the asperity junctions can occur in one of the two bodies depending on the relative magnitude of interfacial adhesion strength and the breaking (shearing) strength of surrounding local regions. Wear fragment results from such shearing whereas no wear occurs when shearing takes place along the interface. In another mechanism, plastic shearing of successive layers of an asperity contact results in detachment of a wear fragment. The detached fragment may be transferred to the mating surface due to adhesion. Further, sliding causes formation of more fragments. The adherence of fragments implies a strong bond between the fragment and the surface while the formation of final loose particles implies a weak bond. Chemical changes in the fragment due to oxidation may reduce adhesive strength and enhance formation of loose particle. Sometimes the residual elastic energy of adherent fragments may be responsible for the formation of loose particles. When captured between two surfaces, the fragment is heavily stressed and as the other surface continues to move, only residual elastic stresses remain. If the elastic energy overcomes adhesive energy in magnitude, a fragment forms a loose wear particle. Severe varieties of adhesive wear are often termed as galling, scuffing, smearing or welding.

Based on experimental data, the amount of wear is usually proportional to the applied load W and the sliding distance x and inversely proportional to the hardness H of the surface being worn away. Thus the volume of wear v is given as [Holm, 1946]

$$v = \frac{kWx}{H} \tag{6.1}$$

where k is a non-dimensional wear coefficient dependent on the material pair and their surface cleanliness. Following the approach of Archard (1953), Eq. (6.1) can be derived. Let us consider two surfaces in a sliding contact under the applied load W. It is assumed that during an asperity interaction, the asperities deform plastically under the applied load, and at each unit event there is a definite probability that a wear particle will be produced. It is also assumed that the contact is made up of asperities with an average radius of a (Fig. 6.1). If the material in an asperity yields under the maximum normal load dW, then

$$dW = \pi a^2 H \qquad (6.2)$$

where H is the mean contact pressure under the condition of full plasticity or hardness of the softer material. Now if it is assumed that this asperity contact produces a wear particle of volume dv and of hemispherical shape with radius equal to the contact radius, then

$$dv = \frac{2}{3}\pi a^3 \qquad (6.3)$$
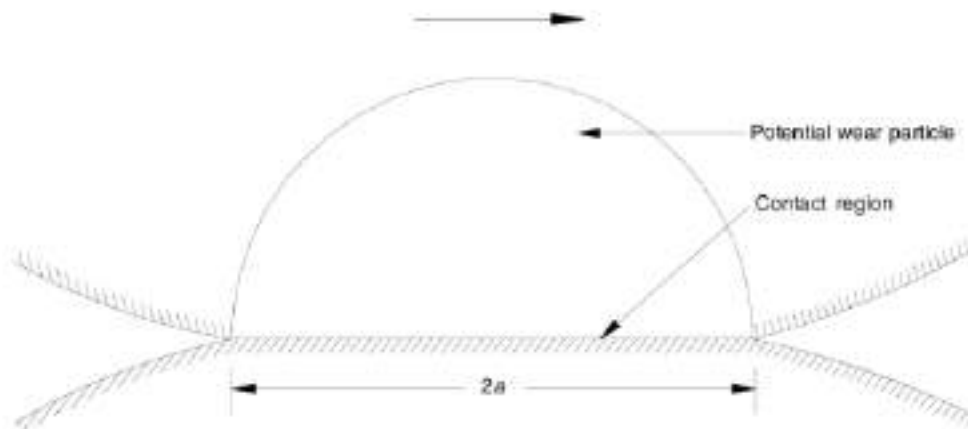
Fig. 6.1 Schematic representation of generation of a hemispherical wear particle during a sliding contact.

Finally, the contact may be assumed to remain in existence for a sliding distance $dx\ (=2a)$, after which it is broken and load is taken up by a new asperity contact.

Therefore,

$$dx = 2a \qquad\qquad (6.4)$$

Using Eqs. (6.2), (6.3) and (6.4),

$$\frac{dv}{dx} = \frac{1}{3}\frac{dW}{H} \qquad\qquad (6.5)$$

If only a fraction (= $3k$) of all encounters produces wear particles, then the volume of wear by all the asperities is

$$v \propto \frac{1}{3}\frac{Wx}{H}$$

$$v = \frac{kWx}{H} \qquad\qquad (6.6)$$

Equation (6.6) is based on plastic contact of asperities and is commonly referred to as Archard's equation of adhesive wear. The term k is interpreted as the probability that a wear particle is formed to a given asperity encounter. Typical value of k ranges from 10^{-8} to 10^{-4} for mild wear and from 10^{-4} to 10^{-2} for severe wear for most material pairs and operating conditions. Thus, from the foregoing analysis, it is evident that wear rate is independent of the apparent area and is directly proportional to the applied load. Also, wear rate (wear volume per unit sliding distance) is independent of sliding velocity. For elastic contacts that occur in interfaces with one of the materials with a low modulus of elasticity or with very smooth surfaces, Eq. (6.6) can be written as (Bhushan, 1996)

$$v = \frac{k'Wx}{E^{*}(\sigma/\beta^{*})} \qquad\qquad (6.7)$$

where E^{*} is the effective modulus of elasticity and s and b^{*} are the composite standard deviation of surface heights and correlation length, respectively, and $k\square$ is a non-dimensional wear coefficient. In an elastic contact, strong adhesion of some contacts can lead to generation of wear particles. Repeated elastic contacts can also fail by surface or subsurface fatigue. Further, in all contacts, contact occurs first at the tip of the asperities, i.e., on the nano-asperities which always deform by plastic deformation irrespective of the deformation of the micro-scale asperities; and the plastic contacts are particularly detrimental form of wear standpoint.

Sometimes wear equation is expressed in terms of the rate of wear depth (d/r mm/s), where t is the sliding time. Equations (6.6) and (6.7) can be rewritten as

$$\frac{d}{t} = \frac{kpV}{H} \qquad \text{(plastic contact)} \qquad (6.8)$$

and

$$\frac{d}{t} = \frac{k'pV}{E^*(\sigma/\beta^*)} \qquad \text{(elastic contact)} \qquad (6.9)$$

where p is the apparent normal pressure $(= W/A_a$, where A_a is the apparent area)
and V is the sliding velocity $(= x/t)$. The rate of wear depth is proportional to the pV factor. In other words, the life of an interface is inversely proportional to the pV factor. This pV factor is used in the selection of material for dry contacts.

Archard's wear equation may be modified in the light of flow pressure or yield pressure under combined normal and shear stresses. In such cases, the flow pressure p is lower than that under a static normal load p_m which is equal to hardness H and is expressed as

$$p = \frac{H}{(1 + \alpha\mu^2)^{1/2}} \qquad (6.10)$$

where α is a constant (about 9) and μ is the coefficient of friction. This expression for the flow pressure when used in Archard's wear equation, it takes the form

$$v = (1 + \alpha\mu^2)\frac{kWx}{H} \qquad (6.11)$$

Rabinowicz (1995) has suggested that the average diameter of a loose wear particle may be given by

$$d = 60,000\frac{W_{adh}}{H} \qquad (6.12)$$

where W_{adh} is the work of adhesion.

It is experimentally found that for many systems, the loss of material by wear is indeed proportional to the sliding distance (and for sliding at constant speed, to the time). Figure 6.2 shows the results of pin-on-ring tests, for a wide range of material combinations under unlubricated conditions in the air. In each case, the wear rate (volume removed per unit sliding distance) is essentially constant for the duration of the test. Abrupt changes in wear rate with increasing load are also found for some materials. Figure 6.3 shows such behaviour. The ferritic stainless steel pin

undergoes a rapid increase in the wear rate above a critical value of load, and below the critical load, the wear rate increases steadily with load. Such an abrupt change is generally attributed to large scale welding and seizure that occur at these higher loads. However, the wear rate of a brass pin sliding on a tool steel ring increases linearly with load as per Archard's wear equation.
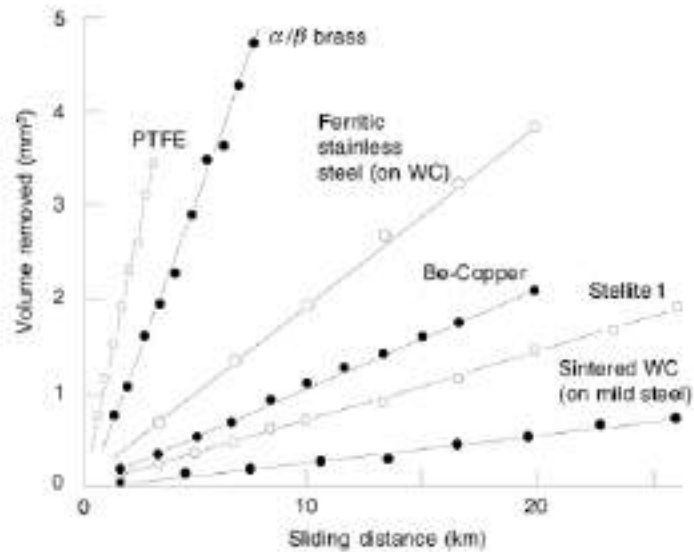
Fig. 6.2 Wear volume against total sliding distance from unlubricated pin-on-ring tests [Archard, 1956].
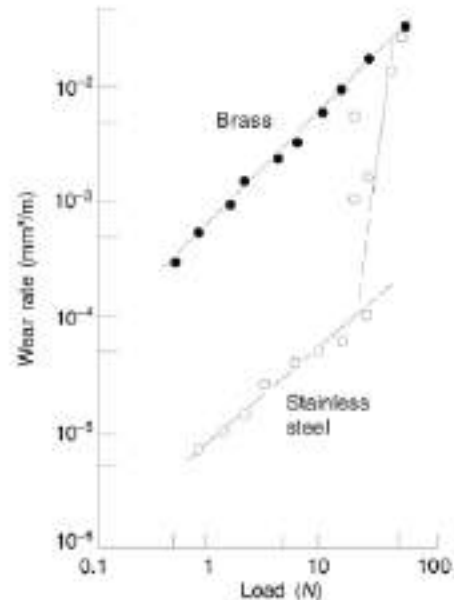
Fig. 6.3 Wear rate against load (logarithmic scales) for brass and ferritic stainless steel pins sliding against tool steel counter-faces in unlubricated pin-on-ring tests [Archard, 1956].

Lubricants and degrees of metallurgical compatibility, which is basically the degree of solid solubility when two metals are melted together, affect wear significantly. The wear coefficient varies by up to two orders of magnitude, depending on the degree of compatibility and by up to three orders of magnitude, depending on the extent of lubrication at the interface. Thus identical metal pairs must be avoided for low wear and friction. Table 6.1 provides some typical comparative values of wear coefficient (k) for metal on metal (both non-hexagonal structure) and non-metal on metal (both with non-hexagonal structure) combinations under different degrees of lubrications. It is found that hexagonal close packed (HCP) metals exhibit low friction and wear than cubic metals as hexagonal metals have a limited number of slip planes responsible for such behaviour. For polycrystalline materials, the one with high grain boundary densities (finer grains) exhibits higher wear rates than those with lower grain boundary densities (coarser grains) or single crystalline materials. The presence of grain boundaries in these materials influences adhesion and, hence friction and wear.

Table 6.1 Typical Values of Wear Coefficients (*k*)

Condition	Metal on metal ($k \times 10^{-6}$)		Non-metal on metal ($k \times 10^{-6}$)
	Like	*Unlike*	
Unlubricated	1500	15–500	1.5
Poor lubrication	300	3–100	1.5
Average lubrication	30	0.3–10	0.3
Excellent lubrication	1	0.03–0.3	0.03

2.9 ABRASIVE WEAR

The term 'abrasive wear' includes two types of wear situation, known as two-body abrasion and three-body abrasion, respectively. In both the cases, a soft surface is ploughed by a relatively hard material. In two-body abrasion a rough hard surface slides against a relatively soft mating surface. In three-body abrasion rough hard particles trapped between the two sliding surfaces cause one or both of them to undergo abrasive wear. Examples of two-body abrasion are grinding, cutting and machining whereas those of three-body abrasion are free abrasive lapping and polishing. In many cases, the wear mechanism at the start is adhesive, which generates wear particles that get sandwiched at the interface, resulting in three-body abrasive wear. In most abrasive wear situations, scratching is seen as a series of grooves parallel to the direction of sliding (ploughing). Depending on the degree of severity, abrasive wear is also termed as scratching, scoring or gouging.

In abrasive wear, material may be removed from a surface by several plastic deformation modes. These include ploughing, wedge formation and cutting. In the ploughing mode, the material is displaced from a groove to the sides and ridges form the sides of the ploughed grooves. These ridges get flattened and finally fracture after repeated loading and unloading cycles. The ploughing process may also cause sub-surface plastic deformation and contribute to the nucleation of sub-surface cracks, which eventually results in the formation of thin wear platelets. In the wedge formation mode, an abrasive tip ploughs a groove and develops a wedge on its front. In the cutting mode, an abrasive tip with large attack angle ploughs a groove and removes the material in the form of ribbon shaped or discontinuous debris particles similar to those formed in a metal cutting process. Schematics of the three deformation modes are illustrated in Fig. 6.4.
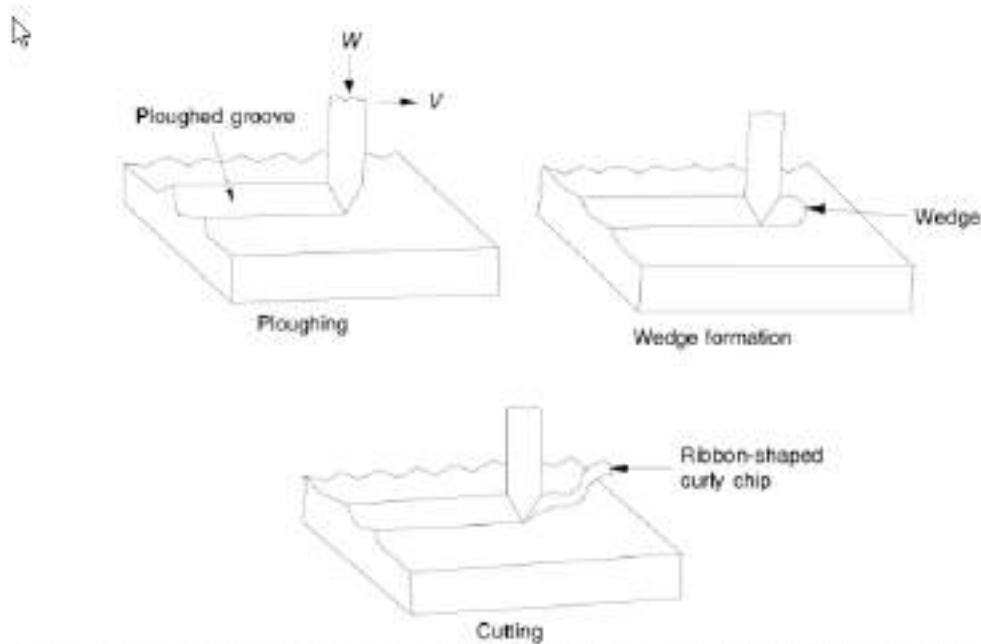
Fig. 6.4 Schematics representation of different deformation modes in abrasive wear processes as a result of plastic deformation.

To obtain a semi-quantitative expression for the abrasive wear for plastic contacts, we consider a simplified model, in which a particle of abrasive has a conical shape, with the attack angle q (Fig. 6.5) and ploughs a track through the softer flat surface with a depth of d and width $2a$. In traversing a distance x, the volume of the material displaced is, $v = axd$. But $d = a \tan q$; therefore, $v = a^2 x \tan q$. We assume that the material has yielded under the normal load W only and thus $W = 1/2 p a^2 H$, where H is the hardness of the softer material. Therefore, the volume of the displaced material may be expressed in terms of load as

$$v = \left(\frac{2W}{\pi H}\right) x \tan \theta \qquad (6.13)$$
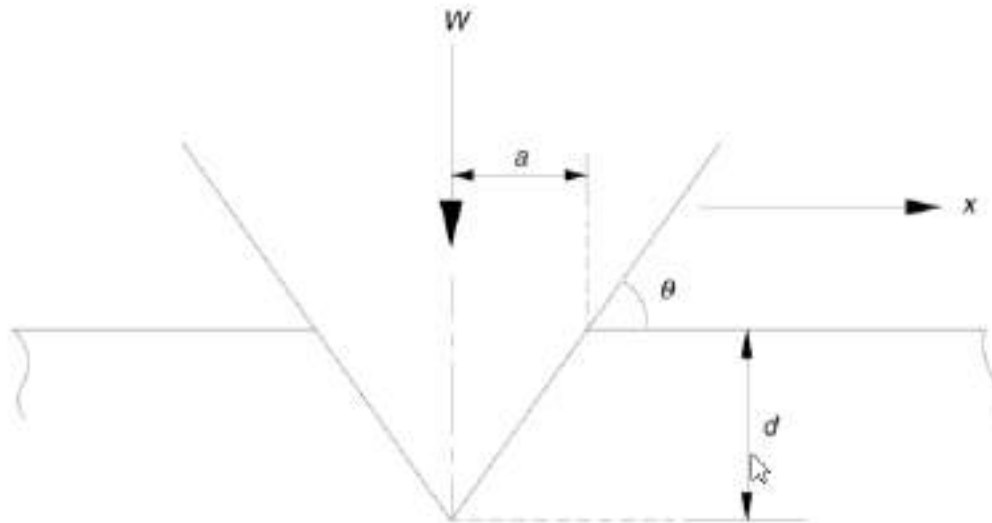
Fig. 6.5 Abrasive wear by a conical indentation.

As with adhesive wear, it is observed that all traversals of abrasive particles do not produce loose wear debris, so Eq. (6.13) is modified to

$$v = k\left(\frac{\tan\theta}{\pi}\right)\frac{Wx}{H} \tag{6.14}$$

where k is the proportion of events which actually result in the formation of a wear particle. An equation of the form similar to Archard's equation for adhesive wear is written as

$$v = \frac{k_{abr}Wx}{H} \tag{6.15}$$

where k_{abr} ($= k \tan q / p$) is a non-dimensional wear coefficient that includes the geometry of the asperities and probability of the formation of wear particle. The value of k_{abr} typically ranges between 10^{-6} and 10^{-1}. The rate of abrasive wear is often very large—two to three orders of magnitude larger than adhesive wear. The derivation of the abrasive wear equation is based on a very simple model where the distribution of asperity heights, shapes and any material build up ahead of the asperities are not considered.

The abrasive wear equation developed for two-body abrasive wear is also valid for three-body abrasive wear with the only difference that k_{abr} is lower by about one order of magnitude. This is because, it is suggested, that many of the particles tend to roll rather than slide. In some conditions, a surface can elastically deform sufficiently to allow the particles to pass through, resulting in minimum damage. Free abrasive polishing is such an example. It is experimentally found that the wear rate in abrasive wear is inversely proportional to hardness and proportional to the normal load and sliding distance. Figure 6.6 shows the mass loss of three ductile metals against the applied load when abraded against an abrasive paper. Mass loss linearly increases with the applied normal load. Wear rate also changes as a function of sliding velocity and the particle size of the abrasive paper. Figure 6.7 shows the dependence of sliding velocity and abrasive grit size for copper being abraded against an SiC abrasive paper. Wear rate increases marginally for a large increase in sliding velocity. With increase in sliding velocity, strain rate increases and yield stress tends to increase. On the contrary, at high sliding velocity, high interface temperature results in a decrease in yield stress. These two counteracting effects make wear rate insignificantly sensitive to sliding velocity. Wear rate increases with grit size initially because of the inclusion of geometry (via tan$g$) of abrasive particle in the wear equation. But at a higher particle size, this effect becomes negligible. Wear rate is also found to be affected by sliding distance, RMS surface roughness and the relative hardness of abrasive medium to workpiece.
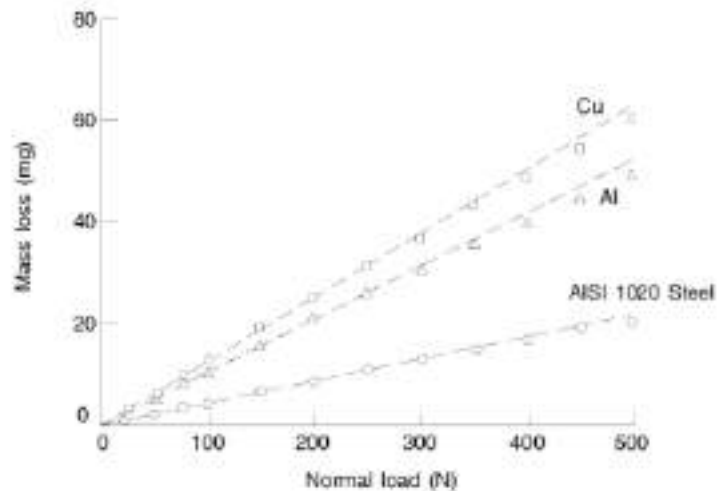
Fig. 6.6 Mass loss of three ductile metals against applied normal load subjected to two-body abrasion by 115 μm SiC abrasive paper [Misra and Finnie, 1981].
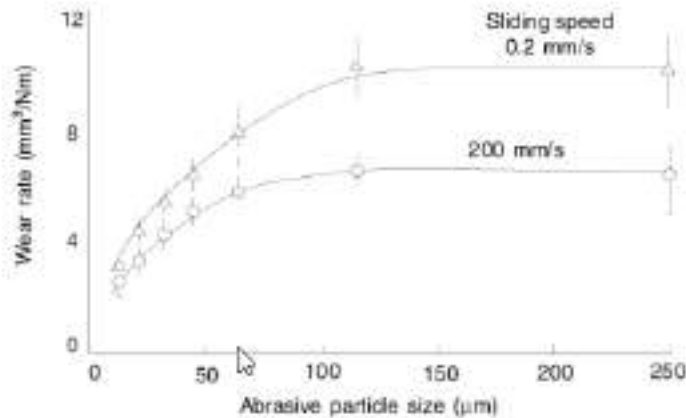
Fig. 6.7 Wear rate of copper, subjected to two-body abrasion by SiC abrasive paper, as a function of abrasive particle size at two different sliding velocities [Misra and Finnie, 1981].

In brittle solids, abrasive wear occurs by brittle fracture. At low loads, sharp asperity contact causes only plastic deformation resulting in wear. Above a threshold load, brittle fracture occurs and wear takes place by lateral cracking. If N asperities contact the surface with each supporting the load W, the volume of wear per unit sliding distance of the interface is given by (Evans and Marshall, 1981)

$$v = \alpha N \frac{(E/H)W^{9/8}}{K_c^{1/2}H^{5/8}} \qquad (6.16)$$

where α is a material-independent constant, E is elastic modulus, H is hardness and K_c is fracture toughness (resistance to fracture). A good correlation has been observed in grinding experiments between wear rate at constant loads and material properties for various ceramic material combinations as predicted by this lateral fracture model.

2.10 CORROSIVE WEAR

Corrosive (or chemical) wear takes place when sliding occurs in a corrosive environment. Corrosive wear in the air is generally called *oxidative wear* as the most dominant corrosive medium in the air is oxygen. The corrosive products (oxides) form a micrometer thick film on the surfaces and sliding action wears it away. In absence of sliding, the film tends to arrest the corrosion. Thus corrosive wear requires both corrosion (chemical reaction) and rubbing (sliding action). The oxide film sometimes

prevents metal–metal contact and thus mitigates against the severe adhesion-enhanced wear, which would otherwise occur. Corrosive wear is important in many industries such as mining, mineral processing, chemical processing, slurry handling.

Oxides of most metals have volumes significantly different from those of their parent metals. So oxide formation causes the development of stresses in the oxide, which increase with film thickness. At some critical film thickness the oxide film can fail either by blistering or by cracking. Blistering takes place when the stress within the film exceeds the strength of the adhesive bond between oxide and substrate. Cracking occurs when the oxide fails in tension. The critical film thickness thus depends on the metal/oxide volume ratio, on the adhesive bond between the oxide and substrate and on the strength of the oxide. When sliding occurs, failure of the oxide film to produce wear debris depends on the stresses resulting from film formation, stresses caused by external normal and tangential loads and thermal stresses induced by flash temperatures at asperity contacts. The stability of the film depends on the hardness of the substrate. A softer substrate deforms plastically and leaves the thin brittle film unsupported.

Archard (1980) has given a simple qualitative development of corrosive wear theory, which shows that the rate of wear (volume of wear per unit sliding distance) can be described again by an equation of the form

$$v = \frac{KW}{H} \qquad 6.17)$$

where the wear coefficient $K = K_3 l/2a$, K_3 is the proportion of events, which produces a wear particle, l is the critical film thickness at which the film becomes unstable and $2a$ is the width of an asperity contact. The values of K_3 and l are dependent on various thermal, mechanical and chemical variables.

Corrosion can take place because of chemical or electro-chemical interaction of the interface with the environment. Chemical corrosion occurs in a highly corrosive environment and is generally enhanced in high temperature and high humidity environments. Electro-chemical corrosion takes place by galvanic action and is influenced by relative electro-potential. Electro-chemical corrosion is accelerated in corrosive environment because corrosive fluids provide a conductive medium for galvanic action to take place.

The effectiveness of oxidation in providing protective films to resist wear can vary dramatically for relatively small changes in rubbing condition. This is because the factors like film thickness, reactivity, etc. are all functions of both time and temperature. Thus mild-to-severe wear transitions may occur suddenly. Figure 6.8 shows a schematic representation (log–log plot) of the variation of wear rate with load for unlubricated carbon steel sliding on carbon steel. At low loads, below the first transition load, T_1, the wear rate is low, the wear debris is removed in the form of oxide and the worn areas have sufficient time to re-oxidize before they make next contact. At T_1, the wear rate changes by more than two orders of magnitude, large wear debris is formed; the surfaces are severely damaged

and roughened. In the range $T_1 - T_2$, there is insufficient time for contacts to re-oxidize between contacts and adhesion-enhanced wear occurs. With increase in load, at the second transition load, T_2, the wear process returns to 'mild' oxidative wear as the temperature effect becomes predominant. This is because the rate of oxidation increases approximately exponentially with the load while the time available for oxidation between the contacts is inversely proportional to the load. Thus, at high loads, greater than T_2, the temperature effect dominates and the oxidation rate increases resulting in 'mild' wear. Also above T_2, the surfaces get a hardened surface layer due to repetitive rapid cooling from high flash temperatures and such hardened layers favour the mild wear regime.
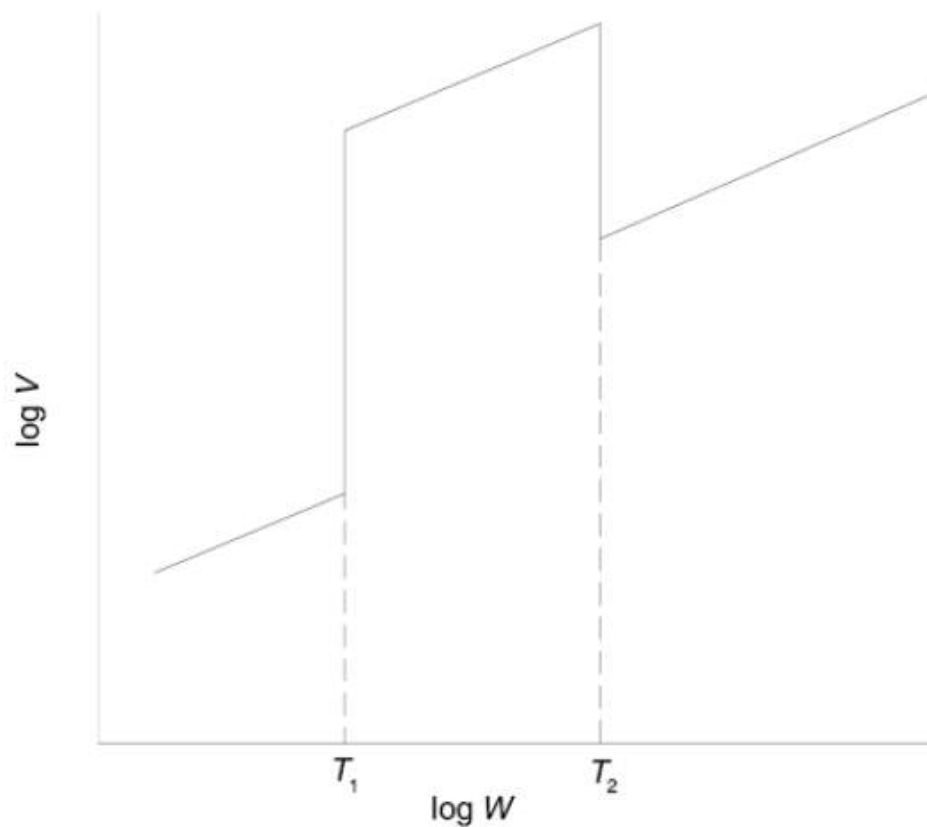
Fig. 6.8 Mild-to-severe wear transitions of an unlubricated steel.

2.11 FATIGUE WEAR

Surface and sub-surface fatigue are observed during repeated sliding and rolling, respectively. Sometimes these are termed as *microscopic* and *macroscopic fatigue wear*. The repeated loading and unloading cycles induce the formation of subsurface or surface cracks, which, after a critical number of cycles, result in the formation of large fragments from the surface and leave large pits in the surface, known as *pitting*. Prior to this final break-up, negligible wear takes place. In this respect, fatigue wear differs markedly from adhesive or abrasive wear where gradual formation of wear particles occurs from the beginning of running. Thus, the amount of material removed by fatigue wear is not crucial, but what is more relevant is the useful life, in terms of numbers of cycles of operation before fatigue failure occurs.

Rolling Contact

Adhesive and abrasive wear mechanisms depend on direct solid–solid contact and these cannot operate if a lubricating film separates the moving surfaces. In well-lubricated rolling element bearings, there is no progressive visible wear due to adhesion or abrasion but bearing life is limited by fatigue. Although no direct contact occurs, the mating surfaces experience large stresses transmitted through the lubricating film during the rolling motion. In the presence of such stresses, the maximum compressive stress occurs at the surface but the maximum shear stress, the position of first yield, occurs at some distance below the surface (Fig. 6.9). As rolling proceeds, the directions of the shear stresses for any element change sign and this is almost entirely responsible for energy dissipation in rolling contacts. If the stress amplitude is above the fatigue limit of the bearing material, fatigue failure will eventually occur. And this is almost invariably the case under the high contact pressures used in rolling element bearings. Since materials in rolling contact applications are often surface hardened, the surface could be brittle. Hence, cracks may also initiate at the surface as a result of tensile stresses and lead to surface fatigue.
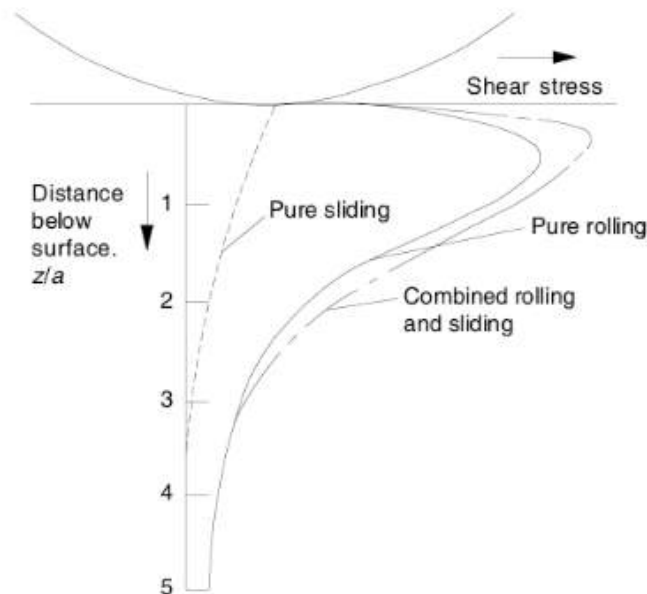
Fig. 6.9 Variation of principal shear stress at various depths directly below the point of contact of two hard surfaces in pure rolling, pure sliding and combined contact.

The life of rolling element bearings (normally referred to as L_{10}) in millions of revolutions for 90% of the bearing population is determined from

$$L_{10} = \left(\frac{C}{W} \right)^p \qquad (6.18)$$

where

p = 3 for point contacts (ball bearings)

= 10/3 for line contacts (roller bearings).

Here C is the basic load capacity of the bearing which is defined as the load that 90% of the bearing can endure for 1 million revolutions under the given running conditions, and W is the equivalent radial or thrust load for radial or thrust bearing, respectively.

Sliding Contact

For sliding contact, wear takes place mainly by adhesion and abrasion. However, asperities can make contact without adhering or abrading and can undergo plastic deformation from the contact stresses. As the deformation continues, cracks may nucleate at and under the surface. With subsequent loading

and deformation, cracks extend and propagate, finally resulting in wear fragment formation at a critical number of contacts. In sliding contact, the maximum shear stress occurs at the surface, which may lead to surface fatigue. Many rolling contacts are frequently accompanied by sliding and the friction stresses due to sliding cause the maximum shear stresses to be nearer the surface (Fig. 6.9) and failure occurs by near surface fatigue. Such failures often occur in hypoid gear teeth, cam roller followers, and wheel-rail contacts and in rolling bearings.

Another type of fatigue known as *static fatigue* is very common in ceramics. Static fatigue results from a stress-dependent chemical reaction between water vapour and the surface of the ceramic. In the presence of tensile stress and water vapour at the crack tip in many ceramics, a chemical induced rupture of the crack-tip bonds takes place rapidly, which increases the crack growth resulting in an increased wear of surface layers both in static and dynamic conditions.

Wear coefficients even for severe wear in most engineering situations are found to be of the order of 10^{-3} to 10^{-7}. In adhesion theory the wear coefficient is simply defined as the probability of a particular asperity contact resulting in the formation of a wear particle. But this interpretation cannot explain the facts that wear coefficients are so low even if adhesion theory assumes that all asperities are plastically deformed and wear particles do form after thousands of cycles of nominally elastic deformation, though all gross plastic deformation of an asperity usually takes place during its first few contacts. If fatigue is considered as the predominant wear mechanism, these facts are easily explained. The explanation may be stated—the wear coefficient may be simply interpreted in terms of the number of fatigue cycles needed to cause the detachment of a wear particle. Thus if the wear coefficient indicates that only 1 in 10^6 asperity contacts results in the formation of wear debris, this means that the stress situation is such that, on an average, it takes 10^6 stress cycles to produce a fatigue fracture. Moreover, although almost all contacts are nominally elastic in the engineering sense, cyclic and sub-surface plastic deformation causes many asperities to fail by fatigue after many cycles of such nominally elastic deformation.

2.12 WEAR TESTING METHODS

Many different experimental arrangements are used to study sliding wear. These are usually carried out either to examine the process by which wear takes place or to simulate practical situations to generate design data on wear rates and coefficients of friction. Close control and monitoring of all the variables which may influence wear are essential if the results of a test are to be useful for wider scientific purposes. Figure 6.12 shows the geometrical arrangements in several common types of wear testing apparatus. For adhesive wear between identical materials, the two surfaces are made of the same material. For abrasive wear testing, one of the surfaces is made of abrasive material, generally the larger one is made of abrasive material. Changes in geometries and arrangements are done for testing of different mechanisms of wear. For two-body abrasive wear, commercial-bonded abrasive paper or cloth is usually used for the counter-face, carrying evenly distributed grit particles of narrow size distribution, bonded to the substrate by a strong resin. In simulating three-body abrasion, silica

(quartz) particles of a narrow size distribution and, from a specified source are fed at a constant rate into the contact region.
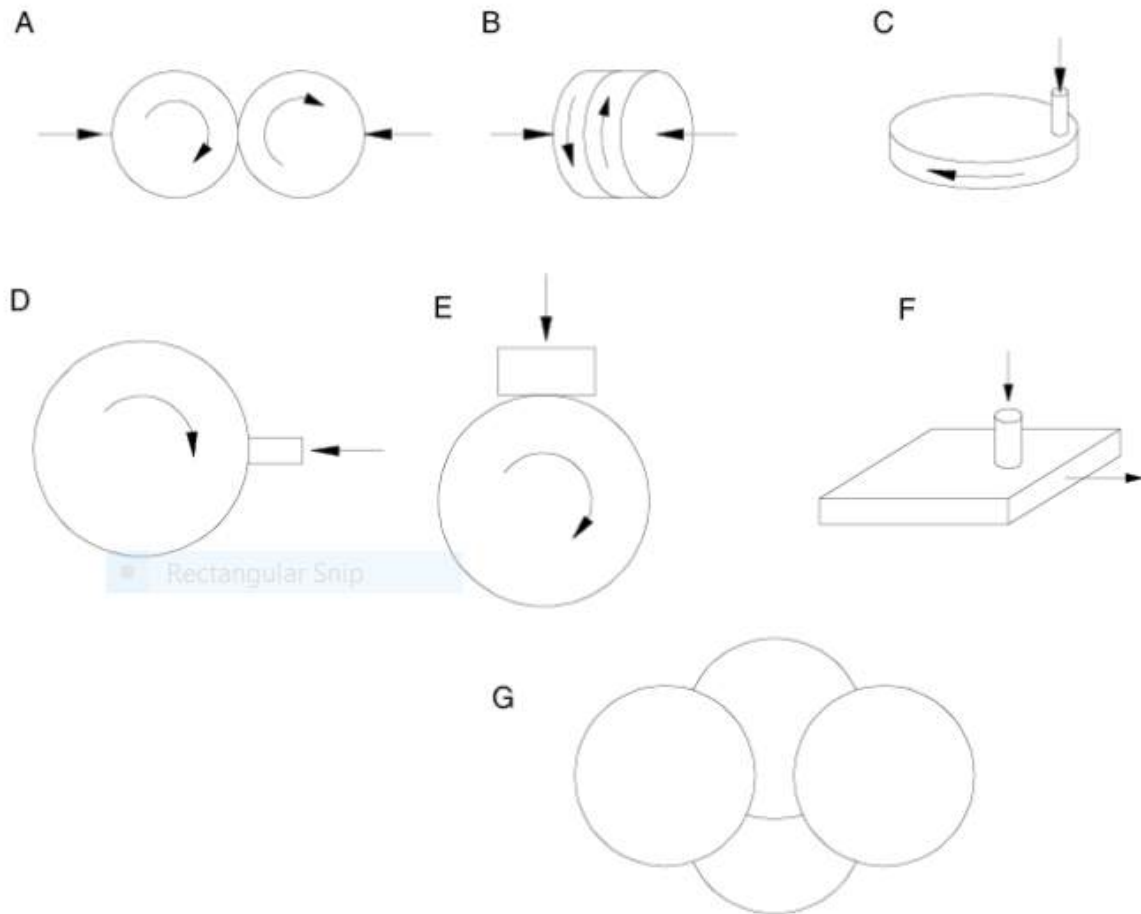
Fig. 6.12   Sliding wear test arrangements.

Figure 6.13 shows schematic diagrams of four types of testing methods for erosive wear. In jet impingement method: (a) particles are accelerated in a fluid stream along a nozzle to strike the target material, which is held some way from the end of the nozzle at a fixed angle. In re-circulating loop test, (b) a two-phase flow of particles and fluid are driven around a loop of pipe-work where the specimen is kept completely immersed in the flow. In centrifugal accelerator, (c) a continuous stream of particles, generated by circular motion of a rotor, strikes the stationary specimens arranged around the rim after rotor. In whirling arm rig, (d) two specimens at the ends of a balanced rotor move at high

speed through a slowly falling stream of particles, striking them at the peripheral speed of the rotor.
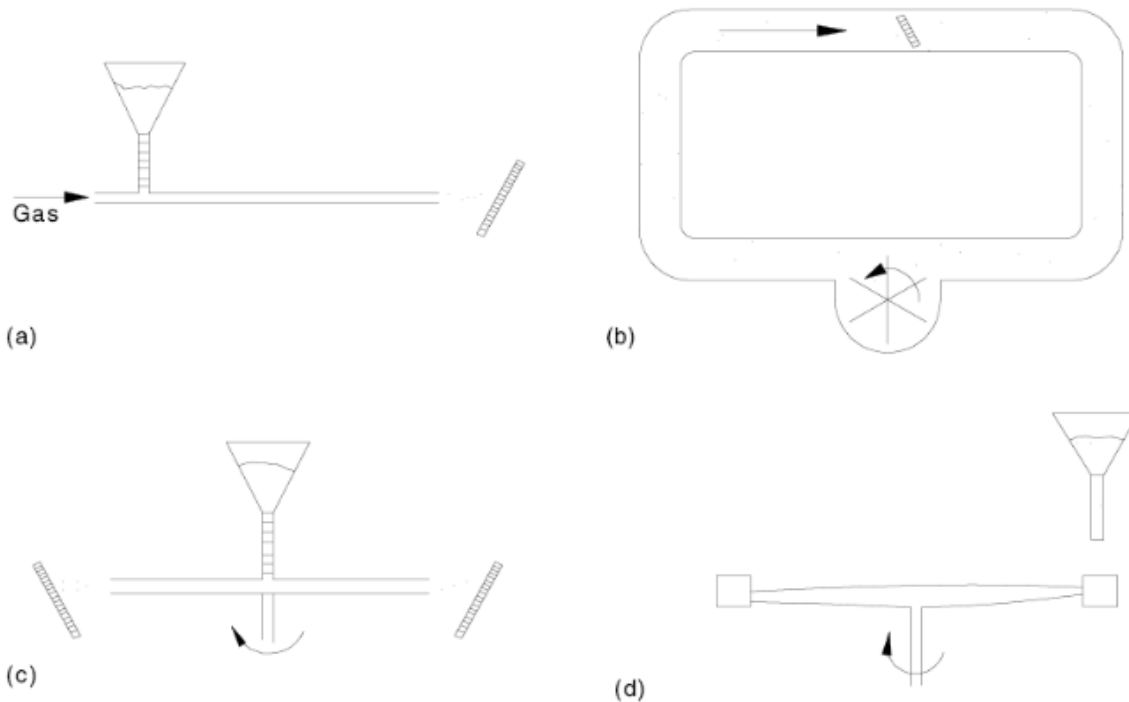
Fig. 6.13   Schematic representation of erosive wear test arrangements: (a) jet impingement method (b) re-circulating loop (c) centrifugal accelerator (d) whirling arm rig.

2.13. WEAR OF METALS

Clean metals and alloys exhibit high adhesion in a solid contact, consequently high friction and wear. The wear rate in high vacuum can be very high. Due to contamination, chemical films are formed; adhesion is reduced resulting in reduction of friction and wear. In metal-to-metal wear tests, high stresses can result in galling and seizure even after a single cycle. To determine galling stress, button and block galling test is performed where new specimens are tested at progressively higher stress levels until galling just starts. Galling usually appears as a groove or a score mark and galling stress acts as a good measure for wear resistance of a given material pair. Table 6.2 shows typical for values of wear coefficients for various similar and dissimilar metals.

Table 6.2 Wear Coefficient for Metal Pairs at Normal Load 20 N and Sliding Velocity 1.8 m/s [Archard, 1953]

Metal pair	Wear coefficient k ($\times 10^{-4}$)	Vickers hardness (kg/mm^2)	
Cd on Cd	57	20	
Zn on Zn	530	38	
Hg on Hg	40	43	
Cu on Cu	110	95	
Pt on Pt	130	138	
M.S. on M.S.	150	158	Hardness value is for the softer material.
Stainless steel on stainless steel	70	217	
Cd on M.S.	0.3	20	
Cu on M.S.	5	95	
Pt on M.S.	5	138	
M.S. on Cu	1.7	95	
Pt on Ag	0.3	43	

Galling data show that identical metal pairs do poorly in terms of wear resistance compared to dissimilar metal couples. Considerable improvement in wear resistance can be achieved when dissimilar metals are paired. Changing the surface characteristics, such as by adding a coating or by surface treatment can also improve wear resistance.

Interface temperature, produced at asperity contacts during sliding of metallic pairs under unlubricated conditions, results in thermal oxidation leading to oxide film formation. The oxidation film can prevent severe wear. At low ambient temperatures, oxidation occurs at asperity contacts from frictional heating. But at higher temperatures, general oxidation of the entire surface occurs and effects wear. Oxidation of iron and many metals follows a parabolic law where the oxide film thickness (h) is related

to time as, $h = ct^{1/2}$ with c is the parabolic rate constant at elevated temperature and t is the average growth time. Since diffusion is thermally activated, growth rate in oxide film thickness during sliding depends on temperature following an Arrhenius type of relation

$$K_p = A \exp\left(\frac{-Q}{RT}\right) \qquad (6.25)$$

where K

p is the parabolic rate constant for growth of the oxide film, A is the parabolic Arrhenius constant for the reaction, Q is the parabolic activation energy associated with oxide, R is the universal gas constant and T is the absolute temperature of the surface. Arrhenius constant for sliding is found to be several orders of magnitude larger than that for static conditions. It means that oxidation under sliding condition is much more rapid than static condition and it may result from increased diffusion rates of ions through a growing oxide film.

The effect of operating conditions, the various regimes of mechanical and corrosive wear of any particular pair of rubbing materials can be shown on a single wear map plotted on axes of normalized pressure (p/H) and sliding velocity. Figure 6.14 shows a wear map for soft carbon steel sliding in the air at room temperature. The map can be divided into regions corresponding to different wear regions with boundaries of contact pressure and sliding speed. This approach is criticized, as it does not take into account the differences of surface shear strength or surface slope. However, many metals show similar wear regime maps. These wear maps are useful in providing guidance for proper selection of materials and performance envelopes for metals.
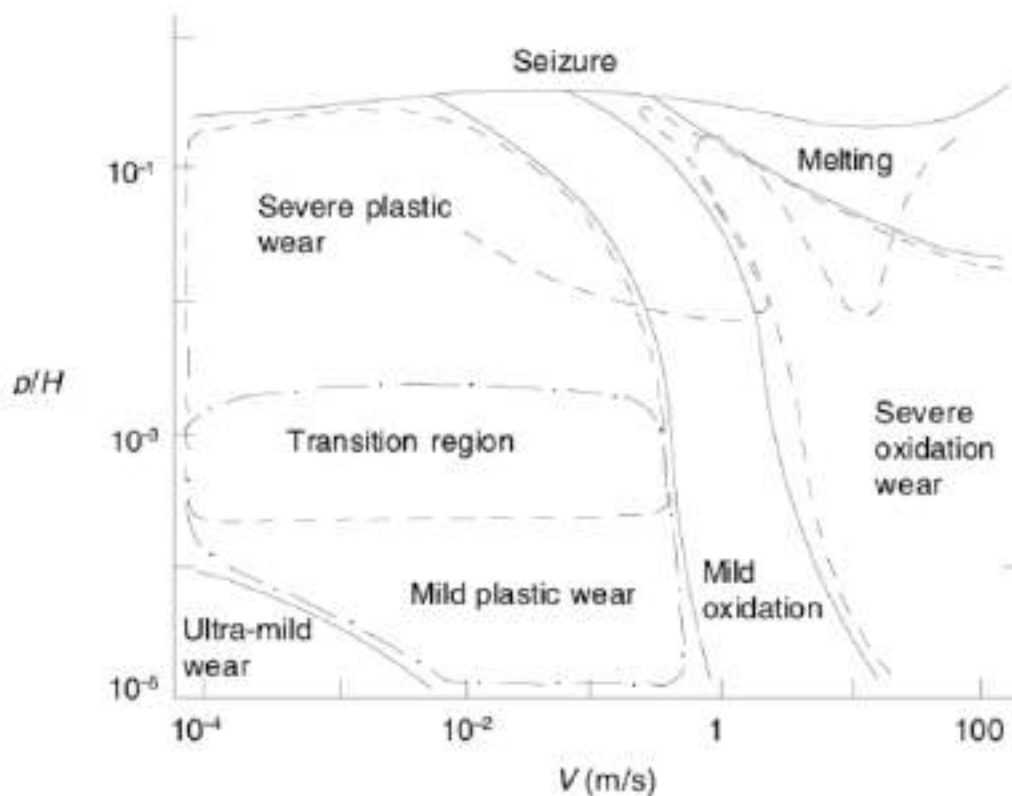
Fig. 6.14 Wear map for soft carbon steels [Lim and Ashby, 1987].

2.14 WEAR OF CERAMICS

Ceramic materials differ from metals in the nature of inter-atomic bonding and this leads to a very limited capacity for plastic flow at room temperature. Compared to metals, ceramics are more inclined to respond to stress by brittle fracture. In oxide ceramics, crack growth is sensitive to environmental factors, which affect the mobility of wear surface dislocations and hence influence plastic flow. Such a chemo-mechanical effect is known as *Rehbinder effect*. Unlubricated sliding of ceramics results in significant tangential forces, which may lead to fracture rather than plastic flow. Sliding wear mechanisms in ceramics can involve fracture, tribo-chemical effects and plastic flow. Transitions between regimes dominated by each of these commonly lead to sharp changes in wear

rate with load, sliding speed or environmental conditions. Mild wear in ceramics is associated with a low-wear rate, smooth surfaces, finely divided wear debris, steady friction traces and mechanisms of wear dominated by plastic flow or tribo-chemical reactions. Severe wear causes higher wear rate along with a rougher surface, angular wear debris, a fluctuating friction trace and mechanisms of wear dominated by brittle inter-granular fracture. Ceramic materials obey the Archard equation well enough. Typical values of non-dimensional wear coefficient for engineering ceramics undergoing severe wear are 10^{-4} to 10^{-2}, which for mild wear are 10^{-6} to 10^{-4}.

Figure 6.15 shows the effect of sliding speed on wear rate in Si_3N_4. At low speed, Si_3N_4 forms a surface layer in the air containing water vapour, and this provides the source for wear debris. Since the shear strength of this layer is lower than the bulk ceramic, the coefficient of friction is lowered. As the speed is raised, the tribo-chemically reacted layer ceases to provide protection and the coefficient of friction rises. The increased surface shear stress causes cracking and a transition occurs from mild wear (tribo-chemical) to severe wear (extensive brittle fracture). Surface roughness increases resulting in the rise in the coefficient of friction. Figure 6.16 shows how similar transition in wear rate takes place in Si_3N_4 influenced by the change in humidity of the surrounding air. In humid environment, Si_3N_4 forms silica and hydrated silica film is formed at the interface. The film being soft with low-shear strength reduces the coefficient of friction and wear rate. Similar drop in wear rate as a function of relative humidity has been observed for SiC. In alumina and zirconia, strong sensitivity to water causes the wear rate to increase; typically tenfold in comparison with dry sliding. In the presence of water, the surface plasticity of these ceramics increases and crack growth is enhanced resulting in higher wear rate. Such a chemically induced fracture pheno-menon is known as *stress corrosion cracking* or static fatigue and the chemomechanical effect in which mechanical properties of many materials change as a result of exposure to many liquids, is known as *Joffe-Rehbinder effect*. For different ceramics, the wear volume and the friction coefficient are found to be dependent on temperatures, but the trend of behaviour is not unique and varies from one ceramic material to other.
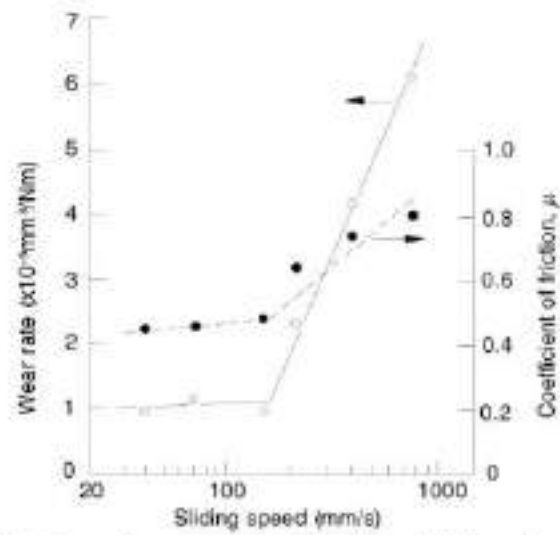
Fig. 6.15 Coefficient of friction and wear rate as a function of sliding velocity of hot-pressed silicon nitride on itself at a normal load of 10 N and ambient air in a pin-on-disk rig [Ishigaki, et al., 1985].
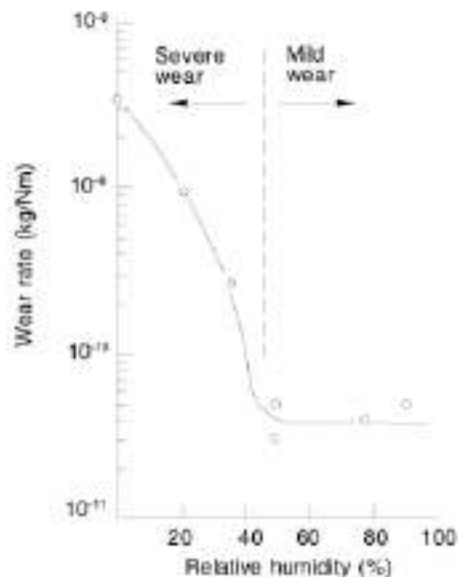
Fig. 6.16 Variation of wear rate with humidity for silicon nitride sliding against itself in a pin-on-disk test in air [Fischer and Tomizawa, 1985].

Ceramic materials respond to conventional lubricants in the same way as metals. Effective lubrication decreases wear rate. However, chemical effects play a significant role even under lubricated conditions. Surface oxidation of Si_3N_4 and SiC occurs even in mineral oils and wear of these ceramics under lubricated conditions is due to tribo-chemical action. Boundary lubricants such as stearic acid function on ionic materials such as Al_2O_3, whereas SiC (with covalent bonding) is not effectively lubricated by stearic acid. Zirconia is susceptible to a phenomenon called thermo-elastic instability where contact between asperities in thin film lubricated sliding causes intense local power dissipation and consequent heating. The local temperature rise significantly distorts the topography of the surface and causes further asperity contact to be concentrated in the same area. This instability results in very high-flash temperatures and rapid wear. Such phenomenon commonly occurs in the lubricated sliding of materials with low-thermal conductivity and high-thermal expansion coefficients. Poor performance of zirconia under some lubricated-sliding conditions is attributed to this phenomenon.

The wear regime maps for ceramics are material specific. Wear maps for Al_2O_3 and Si_3N_4 under dry and paraffin oil-lubricated conditions are shown in Fig. 6.17. The results are from the tests conducted by using a ball-on-three-flats geometry on a four-ball wear tester with identical materials in the air at room temperature. Wear volumes per unit time and various wear mechanisms are also listed

in the figures. The interaction of lubricant with ceramics extends the pressure velocity boundary towards the higher values for a transition from mild-to-severe wear.
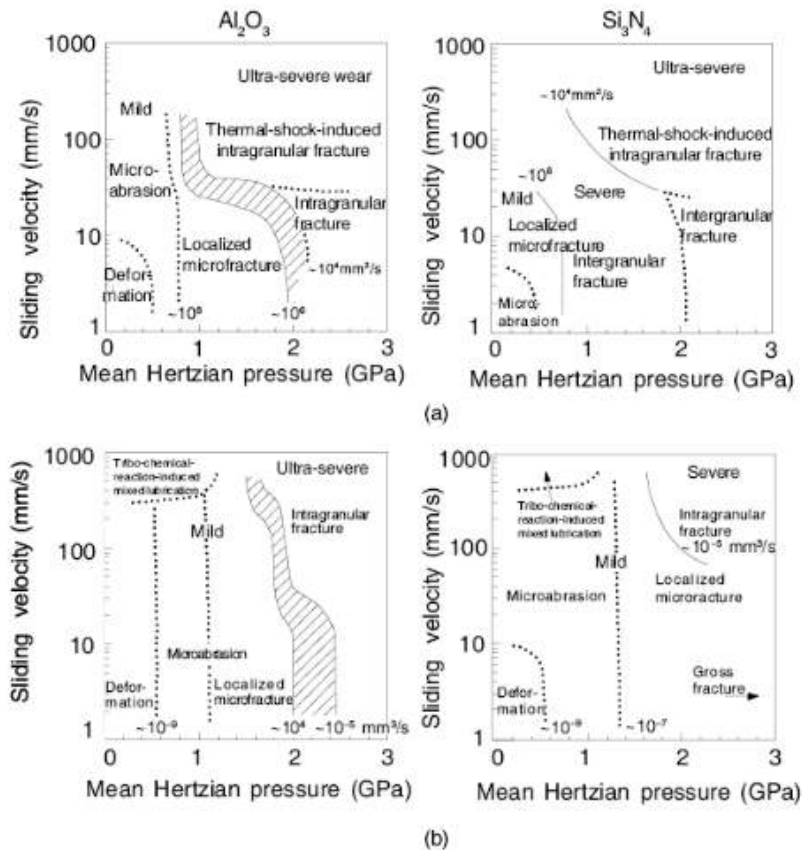
Fig. 6.17 Wear regime maps for Al_2O_3 and Si_3N_4 sliding on themselves at room temperature in a ball-on-three flats geometry on a four-ball wear tester (a) under dry conditions (b) under paraffin oil-lubricated conditions [Hsu and Shen, 1996].

2.15 WEAR OF POLYMERS

Polymers (plastics and elastomers) generally show low friction in comparison to metal and ceramic pairs, but show moderate wear. Dominant wear mechanisms are adhesive, abrasive and fatigue. Adhesive wear occurs if the mating surfaces are smooth. For the cases of sliding of polymers against rough surfaces, the wear primarily occurs by abrasive mechanism. The fatigue mechanism is important in harder polymers such as many thermosetting polymers sliding against smooth surfaces. Asperity deformation in polymers is mainly elastic and wear due to fatigue takes place as a result of

the formation of cracks associated with predominantly elastic deformation. Crack propagation and subsequent intersection of cracks lead to the formation of wear particles.

Polymers flow readily at moderate temperatures and pressures. Thus, polymers and polymer composites are used at lower loads, speed and temperature compared to metals and ceramics. Because of low-thermal conductivities, polymers result in high- interface temperatures, which is a function of the product of normal pressure and sliding velocity (PV). Therefore, polymers are used based on a PV limit, beyond which they start to melt at the interface resulting in rapid increase in wear rate. Polymers have high tolerance to abrasive particles and are generally insensitive to corrosive environments. However, with some fluids, they react with degradation in mechanical properties. In polymers composites, the orientation of the fibres affects the wear rates. The surface roughness of the mating material and its orientation in relation to direction of sliding significantly affects the wear rate. Exposure to the environment also affects mechanical properties as well as friction and wear of polymers. Liquid lubricants interact with polymers in several ways. In some cases, for example in glassy thermoplastics, liquid lubricants cause enhanced plasticity of the surface leading to reduced wear. Again, the same polymer can undergo cracking or stress crazing in other liquids, resulting in greatly enhanced wear.

Figure 6.18 shows the variation of steady-state wear with sliding speed for nylon 6.6 sliding against a smooth, mild steel counter-face under unlubricated conditions. At high-sliding speed, transition from 'mild-to-severe' wear occurs at a speed when the flash temperature is sufficient for softening of the polymer. The arrow indicates the speed at which the calculated flash temperature reaches 250°C, the softening point of the polymer.

2.16 SYSTEMS APPROACH TO WEAR REDUCTION

When surfaces are in relative motion, wear cannot be completely eliminated. It can only be reduced to an insignificant level. If the rate of expected wear is unacceptable, a designer should change the system in some possible way so as to reduce wear. The wear rate in a particular system is governed by the interaction of many factors, which can be recognized and divided into two groups:

(a) The structure of the mechanical system.
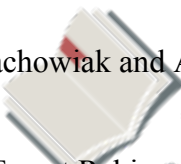
(b) The operating variables.

The structure is described by the materials making up the surfaces in relative motion, the nature of any material present at the interface and the environment. The operating variables include the conditions imposed on the system during operation such as load, speed, temperature, etc. All these factors influence the wear rate and the designer can control most of them. Wear in a system can be reduced/controlled by changing the operating variables, by proper lubrication and by suitable selection of materials and their surface properties. All these are performed in the so-called systems approach to wear analysis.

Questionnaires

1. What is friction and wear?. Explain briefly

2. Explain different friction measurement methods with suitable sketch

3. Explain the different friction theories.

4. Briefly explain friction of metals and non metals

5. Classify the wear and explain briefly

6. Explain the wear mechanisms.

Further Reading:

1. "Tribology, Friction and Wear of Engineering Material", I. M.Hutchings, Edward Arnold, London,1992.

2."Engineering Tribology", G. W. Stachowiak and A. W. Batchelor, Butterworth- Heinemann,1992.

3. "Friction and Wear of Materials", Ernest Rabinowicz, John Wiley & sons,1995.